16. WHOLE-CORE *P*-WAVE VELOCITY AND GAMMA RAY ATTENUATION LOGS FROM LEG 108 (SITES 657 THROUGH 668)[1]

P. J. Schultheiss,[2] J. Mienert,[3] and Shipboard Scientific Party[4]

ABSTRACT

Compressional or primary wave velocity logs (*P*-wave logs) and Gamma Ray Attenuation logs are presented for many of the cores recovered on Leg 108 with the advanced piston corer (APC). The velocity data was collected using a new whole-core logging device that was integrated with the old tracking system of the Gamma Ray Attenuation and Porosity Evaluator (GRAPE). The logs show that it is possible to obtain the fine-scale velocity structure through most soft sediment sequences. This information is needed to help with the detailed cross-correlation of offset holes at each site. Good data cannot be obtained from cores that do not fill the liner completely or from cores with the liner badly damaged.

INTRODUCTION

During Leg 108, continuous curves (or logs) of the *P*-wave velocity data were obtained routinely for the first time in the history of ocean drilling. These logs were obtained by using new equipment, the *P*-wave logger (PWL), developed at the Institute of Oceanographic Sciences specifically for logging the *P*-wave velocity of soft sediment cores within plastic liners. The logs enable us to provide detailed cross-correlation of offset holes at the same site. Logs of this type also help to identify sedimentary features rapidly (e.g., slumps and turbidites) and provide (together with the Gamma Ray Attenuation and Porosity Evaluator [GRAPE]) the detailed density and velocity profiles required to generate accurate synthetic seismograms that can be correlated with seismic profiles. This chapter presents the PWL and GRAPE logs in a graphical format so that the overall quality and nature of the data for any particular site, hole, core, or even section can be seen. This chapter complements contributions from Bloemendal, Tauxe, Valet, et al. (this volume), which provide downhole plots of all whole-core susceptibility logs obtained during Leg 108.

THE PWL AND GRAPE

The application and use of the GRAPE for determining the bulk density of sediments has been discussed extensively in various DSDP volumes (e.g., Evans, 1965; Evans and Cotteral, 1970; and Boyce, 1973 and 1976) and will not be repeated here.

A complete description of the PWL will be given in *Proc., Final Repts. (Pt. B), ODP*, 108. However, as the equipment is new, a brief description of the fundamental workings of this logger is provided here.

The PWL consists of two main units: the transducer assembly and the electronics rack. Two spring-loaded, ultrasonic compressional-wave transducers (500 kHz) are used for transmitting and receiving pulses across the diameter of each section as it passes through the transducer assembly. During Leg 108, the transducer assembly was mounted adjacent to the GRAPE so that the tracking system served both logging systems. Variations in the core diameter were monitored using two displacement transducers mounted behind the ultrasonic transducers. A good ultrasonic coupling was maintained between the core liner and the transducers by a film of water that was sprayed onto the core liner before each logging operation. The electronics rack provided the driving signal to the transmitter and measured the time delay before the arrival of the received pulse. The time delay, core diameter, and pulse amplitude were fed directly to a computer for data handling and storage. The pulse timing was not affected adversely by large changes in signal strength because a zero-crossing, pulse-detecting system was employed with a resolution of 50 ns. This corresponds to a velocity resolution of about 1.5 m/s. The sediment velocity was computed after corrections for traveltime through the liner, the temperature of the sediment, electronic delays, and the time between onset of the pulse and the detected zero crossing. Velocity was displayed in real time on both a television monitor and a hard-copy plotter as a velocity log and, finally, was stored on a floppy magnetic diskette.

The sampling interval along the length of each section depended on the speed of the tracking system and the number of individual samples averaged. During Leg 108, samples were normally taken at 2-cm intervals, after averaging 200 individual pulses.

[1] Ruddiman, W., Sarnthein, M., Baldauf, J., et al., 1987. *Proc., Init. Repts. (Pt. A), ODP*, 108.

[2] Institute of Oceanographic Sciences, Brook Rd., Wormley, Godalming, Surrey, GU8 5UB, United Kingdom.

[3] Woods Hole Oceanographic Institution, Woods Hole, MA 02543, and Geologisch Paläontologisches Institut, Universität Kiel, Olshausenstrasse 40, D-2300 Kiel, Federal Republic of Germany.

[4] William Ruddiman (Co-Chief Scientist), Lamont-Doherty Geological Observatory, Palisades, NY 10964; Michael Sarnthein (Co-Chief Scientist), Geologisch-Paläontologisches Institut, Universität Kiel, Olshausenstrasse 40, D-2300 Kiel, Federal Republic of Germany; Jack Baldauf, ODP Staff Scientist, Ocean Drilling Program, Texas A&M University, College Station, TX 77843; Jan Backman, Department of Geology, University of Stockholm, S-106 91 Stockholm, Sweden; Jan Bloemendal, Graduate School of Oceanography, University of Rhode Island, Narragansett, RI 02882-1197; William Curry, Woods Hole Oceanographic Institution, Woods Hole, MA 02543; Paul Farrimond, School of Chemistry, University of Bristol, Cantocks Close, Bristol BS8 1TS, United Kingdom; Jean Claude Faugeres, Laboratoire de Géologie-Océanographie, Université de Bordeaux I, Avenue des Facultés Talence 33405, France; Thomas Janacek, Lamont-Doherty Geological Observatory, Palisades, NY 10964; Yuzo Katsura, Institute of Geosciences, University of Tsukuba, Ibaraki 305, Japan; Hélène Manivit, Laboratoire de Stratigraphie des Continents et Océans, (UA 319) Université Paris VI, 4 Place Jussieu, 75230 Paris Cedex, France; James Mazzullo, Department of Geology, Texas A&M University, College Station, TX 77843; Jürgen Mienert, Geologisch-Paläontologisches Institut, Universität Kiel, Olshausenstrasse 40, D-2300 Kiel, Federal Republic of Germany, and Woods Hole Oceanographic Institution, Woods Hole, MA 02543; Edward Pokras, Lamont-Doherty Geological Observatory, Palisades, NY 10964; Maureen Raymo, Lamont-Doherty Geological Observatory, Palisades, NY 10964; Peter Schultheiss, Institute of Oceanographic Sciences, Brook Road, Wormley, Godalming, Surrey GU8 5UG, United Kingdom; Rüdiger Stein, Geologisch-Paläontologisches Institut, Universität Giessen, Senckenbergstrasse 3, 6300 Giessen, Federal Republic of Germany; Lisa Tauxe, Scripps Institution of Oceanography, La Jolla, CA 92093; Jean-Pierre Valet, Centre des Faibles Radioactivités, CNRS, Avenue de la Terrasse, 91190 Gif-sur-Yvette, France; Philip Weaver, Institute of Oceanographic Sciences, Brook Road, Wormley, Godalming, Surrey GU8 5UG, United Kingdom; Hisato Yasuda, Department of Geology, Kochi University, Kochi 780, Japan.

P-WAVE VELOCITY LOGS

Each hole is presented as a separate figure in 30-m sections (Figures 1 through 23). Depth in meters below seafloor (mbsf) is plotted on the *Y*-axis, which is marked by ticks at 1-m intervals. The depth range for 0 to 30 m, 30 to 60 m, etc., is shown beneath each 30-m profile. The *P*-wave velocity (corrected to 20°C) is plotted on the *X*-axis. A 100-ms^{-1} scale bar is shown at the top and bottom of each 30-m section. The scale bar is actually 1500 to 1600 ms^{-1}. Each core was plotted by assigning the depth below seafloor of the top of the core (taken from the coring summary) to the top of Section 1. Subsequent sections are assumed to be at multiples of 1.5 m beneath this value. Large gaps in the records generally occur where no core was recovered. However, some gaps occur where sections were not logged successfully because of distorted liners, or where significant air gaps occurred between the inside of the core liner and the sediment. Gaps in the logs (greater than 1 m) that occur because no core was recovered are shown by a vertical line. Logs are presented for most APC cores recovered. Data obtained from cores recovered using the XCB are generally poor because of the higher degree of core disturbance and because a gap often occurred between the inside of the liner and the sediment core.

BULK-DENSITY LOGS

Bulk-density profiles, calculated from gamma-ray-attenuation logs, are presented for each hole as a separate figure and are divided into 9.5-m sections (Figures 3B, 6B, 8B, 10B, 15B, 18B, 20B, and 21B). Each 9.5-m profile is marked at 100-cm intervals. Bulk density is plotted on the *X*-axis using either a 1.2 to 2 g/cm^{-3} or a 1.3 to 2 g/cm^{-3} scale, which is marked at 0.1-g/cm^{-3} intervals. Gaps in the profiles generally occur where sections were not successfully logged because of either (1) cracked or distorted liners, (2) significant amounts of air between the sediment core and the liner, or (3) liners void of sediment. Air between the liner and the sediment core causes a significant apparent decrease in the sediment density because of decreased sediment thickness.

Bulk-density logs are presented for most of the A-holes where the APC was used. Data for Sites 657, 658, and 668 exist only in raw, unprocessed, digitized form and are not presented here.

SITE 657

Site 657 was the first site logged using the new PWL system. The sampling interval was set at 2 mm for this site but was changed to 2 cm for subsequent sites without decreasing quality of the data.

SITE 658

A significant amount of free gas in most of the cores recovered from Site 658 resulted in obtaining little data. Even very small amounts of free gas cause ultrasonic compressional waves that are highly attenuated. Consequently, no data are presented for this site.

SITE 659

Bulk density increases from about 1.6 to 1.9 g/cm^{-3} from Cores 108-659A-1H through 659A-27X (a gradient of approximately 0.0012 $g/cm^{-3}/m^{-1}$). Bulk-density fluctuations have amplitudes on the order of 0.1 g/cm^{-3} over depths of tens of centimeters.

SITE 660

Bulk density increases from about 1.4 to 1.65 g/cm^{-3} from Cores 108-660A-1H through 108-660A-13H (a gradient of approximately 0.002 $g/cm^{-3}/m^{-1}$). An abrupt decrease in density from about 1.65 to 1.35 g/cm^{-3} occurs at about 120 mbsf. Below this depth, density remains at this low value. This boundary also is observed in other index properties (see "Site 660" chapter, this volume).

SITE 661

Bulk density increases from about 1.4 to 1.75 g/cm^{-3} from Cores 108-661A-1H through 108-661A-32X (a density gradient of approximately 0.0012 $g/cm^{-3}/m^{-1}$).

SITE 662

Bulk density increases from about 1.4 to 1.7 g/cm^{-3} from Cores 108-662A-1H through 108-662A-21H (a density gradient of approximately 0.0014 $g/cm^{-3}/m^{-1}$).

SITE 663

Bulk density increases from about 1.4 to about 1.7 g/cm^{-3} from Cores 108-663A-1H through 108-663A-16H (a density gradient of approximately 0.002 $g/cm^{-3}/m^{-1}$).

SITE 664

Bulk density increases from about 1.45 to 1.85 g/cm^{-3} from Cores 108-664B-1H through 108-664B-26H (a density gradient of approximately 0.0016 $g/cm^{-3}/m^{-1}$).

Core 108-664A-1H was shot accidentally below the mud line because of a miscount in the number of pipe stands. This core will be used for detailed study of the correlation between various sedimentological parameters and *P*-wave velocity. Figure 14 shows four logs obtained from the complete core measured across four different axes, as labeled beneath each log. The close correlation between logs illustrates the repeatability and validity of the PWL system, despite axial asymmetries down the length of the core. A complete log for Hole 664D could not be obtained because of on-board time constraints. Consequently, a significant number of gaps occur in the log for this hole (Fig. 17).

SITE 665

Bulk density increases from about 1.4 to 1.7 g/cm^{-3} from Cores 108-665A-1H through 108-665A-9H (a density gradient of approximately 0.0035 $g/cm^{-3}/m^{-1}$). A distinct decrease in density occurs between Cores 108-665A-9 and 665A-11H from 1.7 to 1.45 g/cm^{-3}. Other index properties show similar trends (see "Site 665" chapter, this volume).

SITE 666

Bulk density increases from about 1.45 to 1.7 g/cm^{-3} from Cores 108-666A-1H through 108-666A-12H (a density gradient of approximately 0.0022 $g/cm^{-3}/m^{-1}$).

SITE 667

Bulk density increases from about 1.45 to 2.0 g/cm^{-3} from Cores 108-667A-1H through 108-667A-41X (a density gradient of approximately 0.0014 $g/cm^{-3}/m^{-1}$).

An example of the type of PWL data obtained from cores recovered using the XCB, as opposed to the APC, is shown in Figure 21 for Hole 667A. The data up to 210 mbsf were obtained from cores recovered using the APC, whereas below 210 mbsf, cores were recovered using the XCB. Clearly, discrete measurements performed at selected intervals is preferable when the XCB is used.

ACKNOWLEDGMENTS

We would like to thank S. D. McPhail for designing the electronic systems for the *P*-wave logger, which have been the keystone to its success, and D. Sims for his perseverance in running the *P*-wave logger and GRAPE equipment during the night shift of Leg 108. We thank G. Jones, W. B. Curry, and K. Takahashi for their helpful reviews.

REFERENCES

Boyce, R. E., 1973. Appendix I. Physical property methods. *In* Edgar, N. T., Saunders, J. B., et al., *Init. Repts. DSDP*, 15: Washington (U.S. Govt. Printing Office), 1115–1128.

________, 1976. Appendix I. Definitions and laboratory techniques of compressional sound velocity parameters and water content, wet-bulk density, and porosity parameters by gravimetric and gamma-ray-attenuation techniques. *In* Schlanger, S. O., Jackson, E. D., et al., *Init. Repts., DSDP*, 33: Washington (U.S. Govt. Printing Office), 931–958.

Evans, H. B., 1965. GRAPE - a device for continuous determination of material density and porosity. *Trans., SWPLA 6th Annu. Logging Symp.*, 2:B1–B25.

Evans, H. B., and Cotteral, C. H., 1970. Gamma-ray-attenuation density scanner. *In* Peterson, M.N.A., Edgar, N. T., et al., *Init. Repts. DSDP*, 2: Washington (U.S. Govt. Printing Office), 440–442.

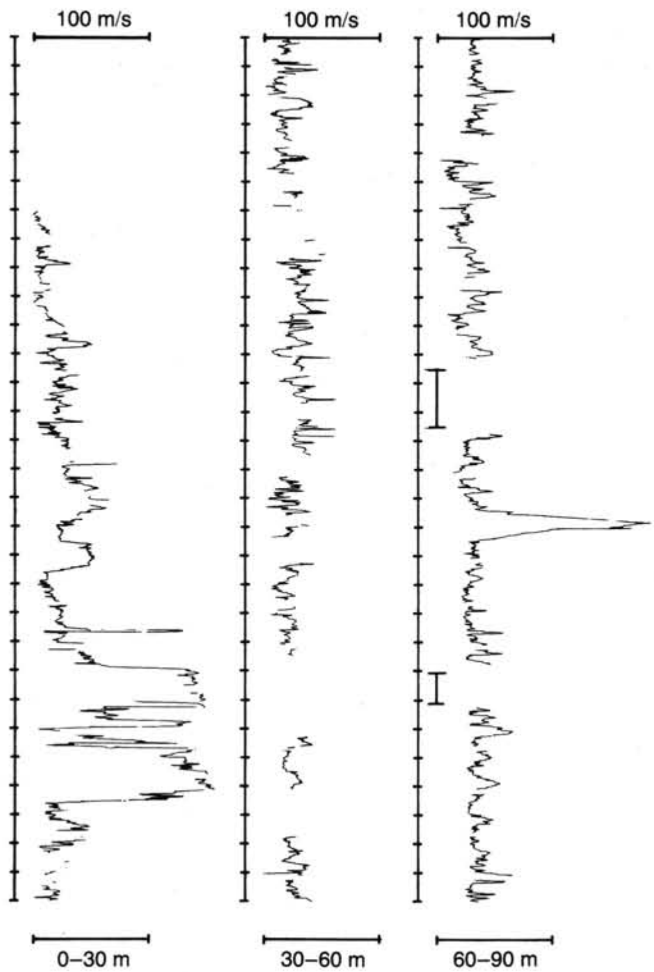

Figure 1. *P*-wave log for Hole 657A.

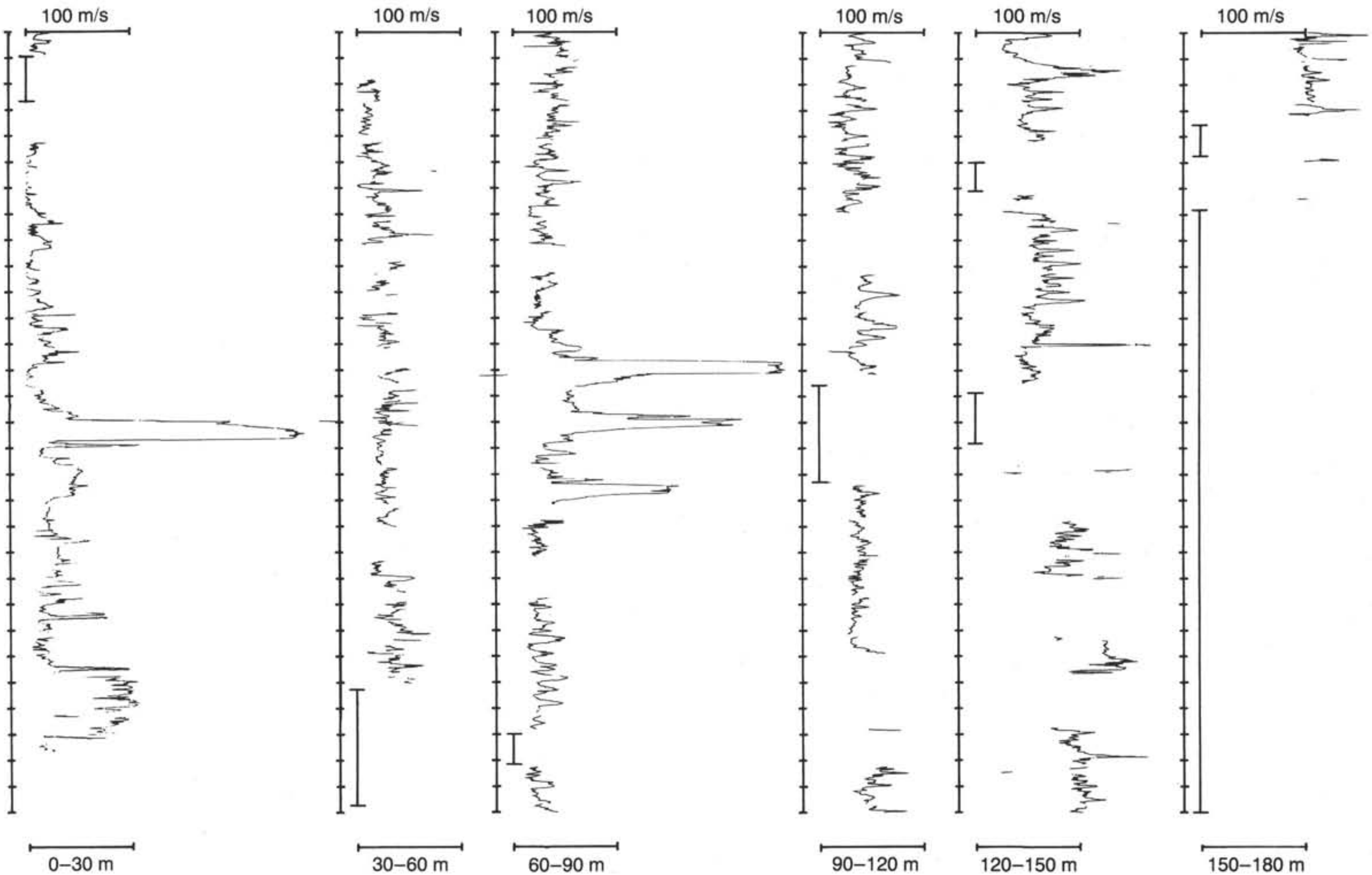

Figure 2. *P*-wave log for Hole 657B.

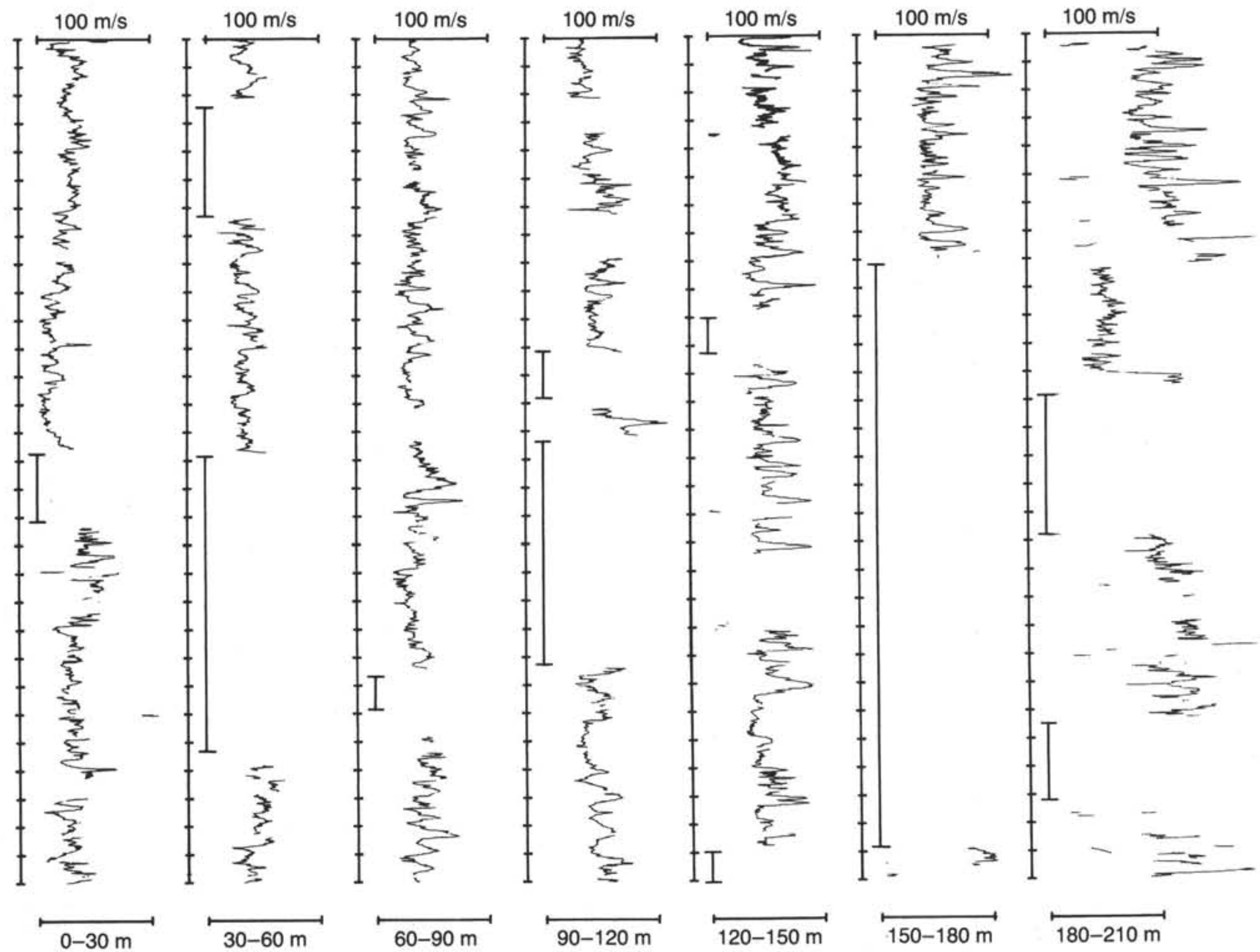

Figure 3A. *P*-wave log for Hole 659A.

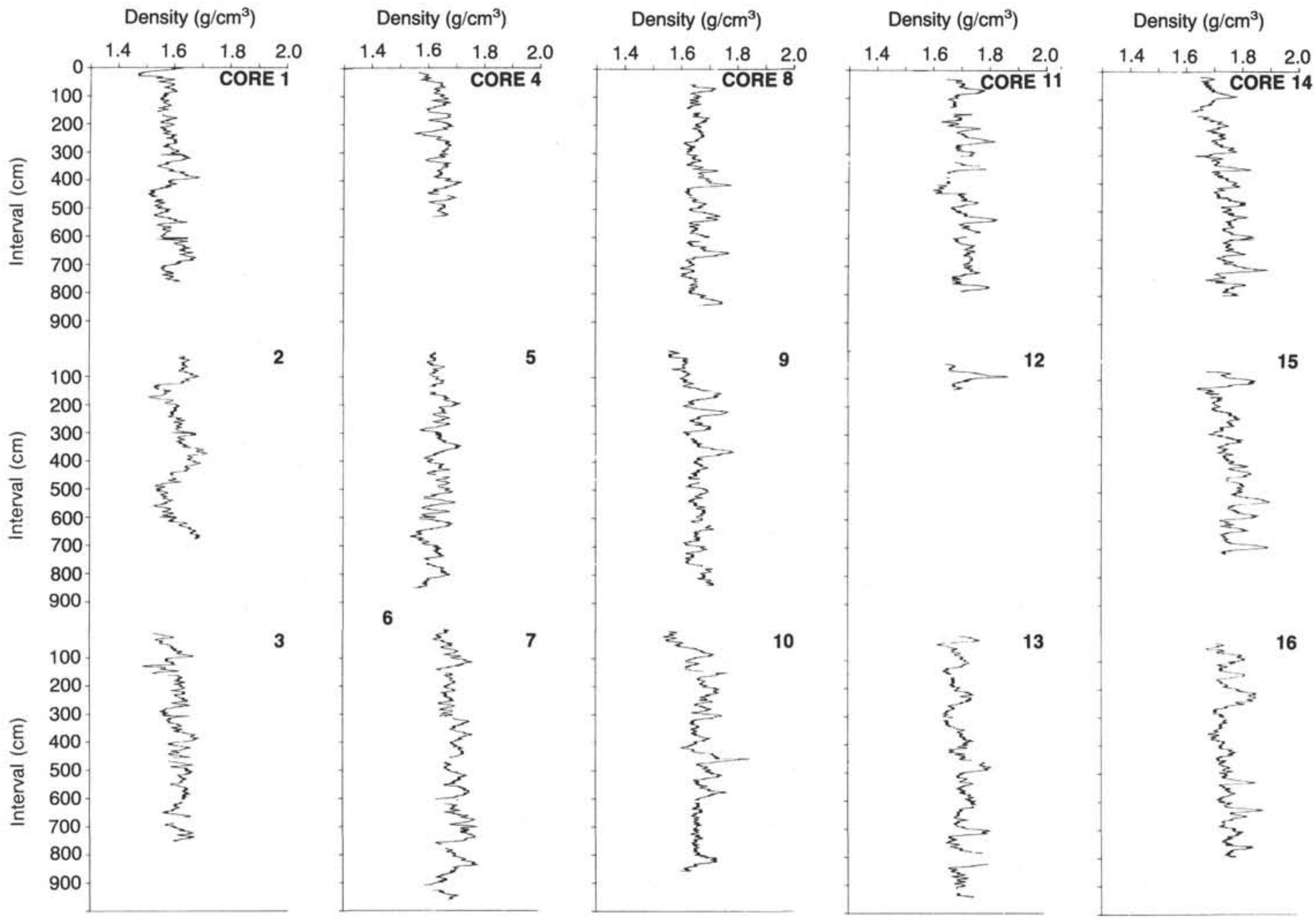

Figure 3B. Bulk-density log for Hole 659A.

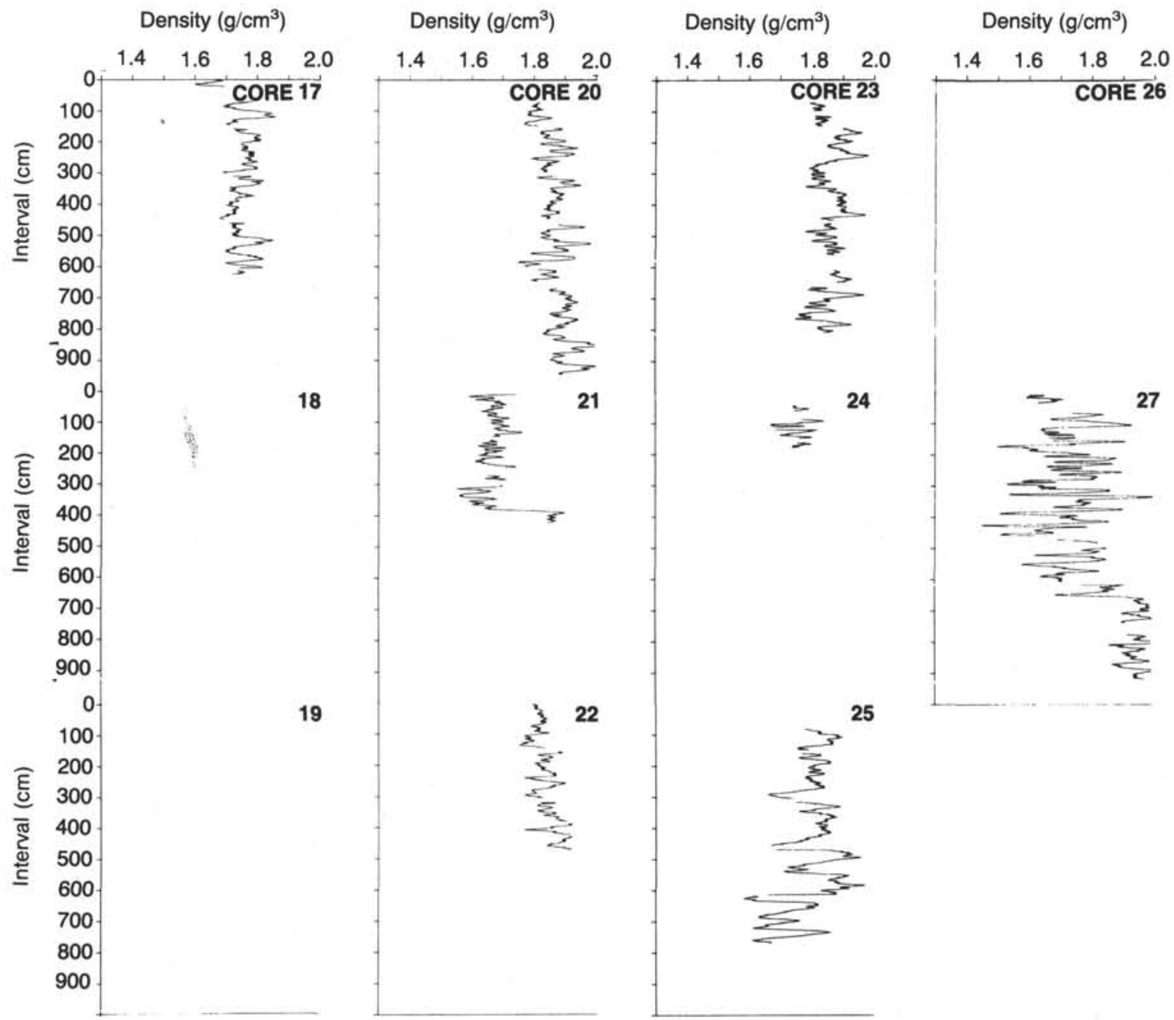

Figure 3B (continued).

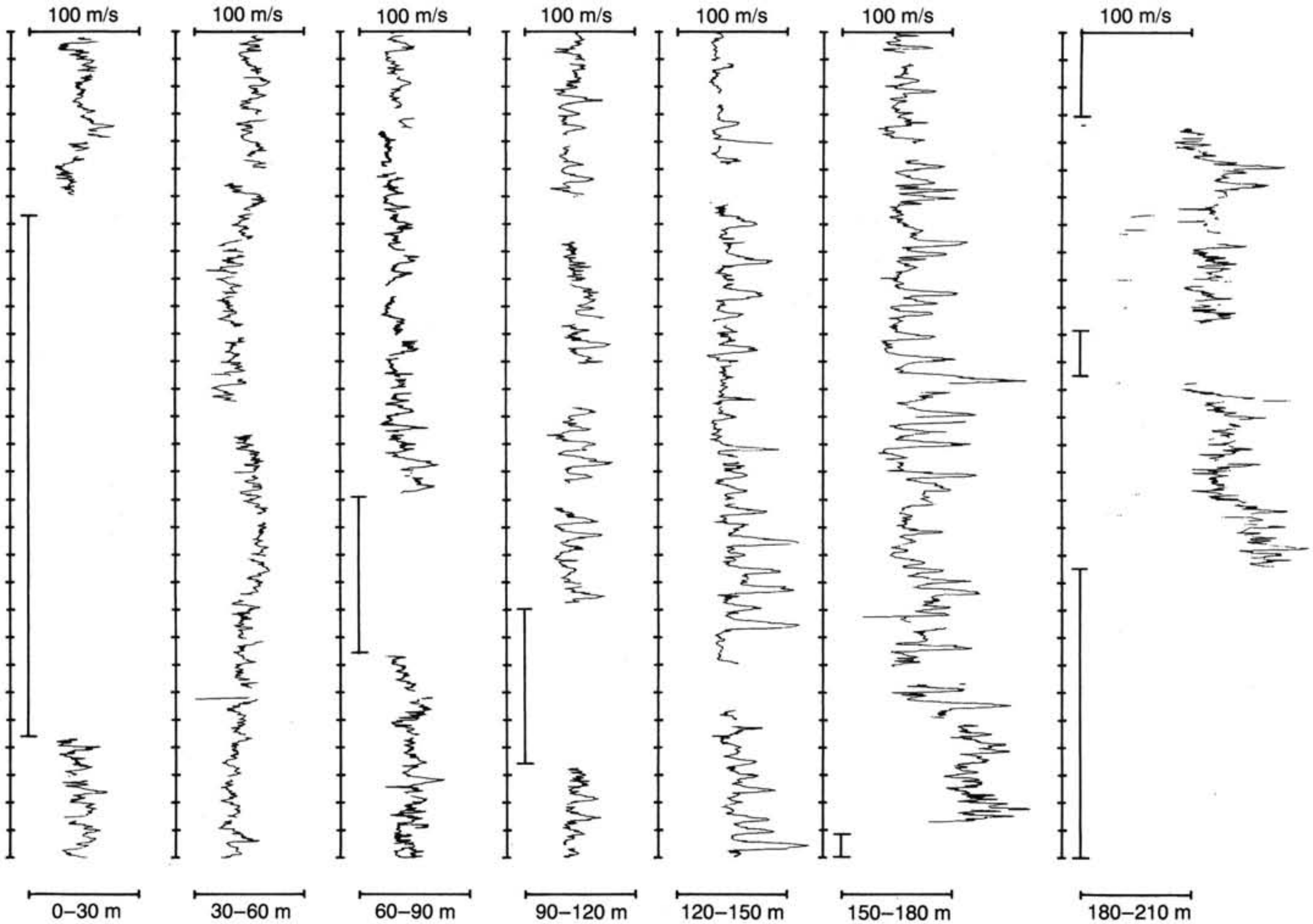

Figure 4. *P*-wave log for Hole 659B.

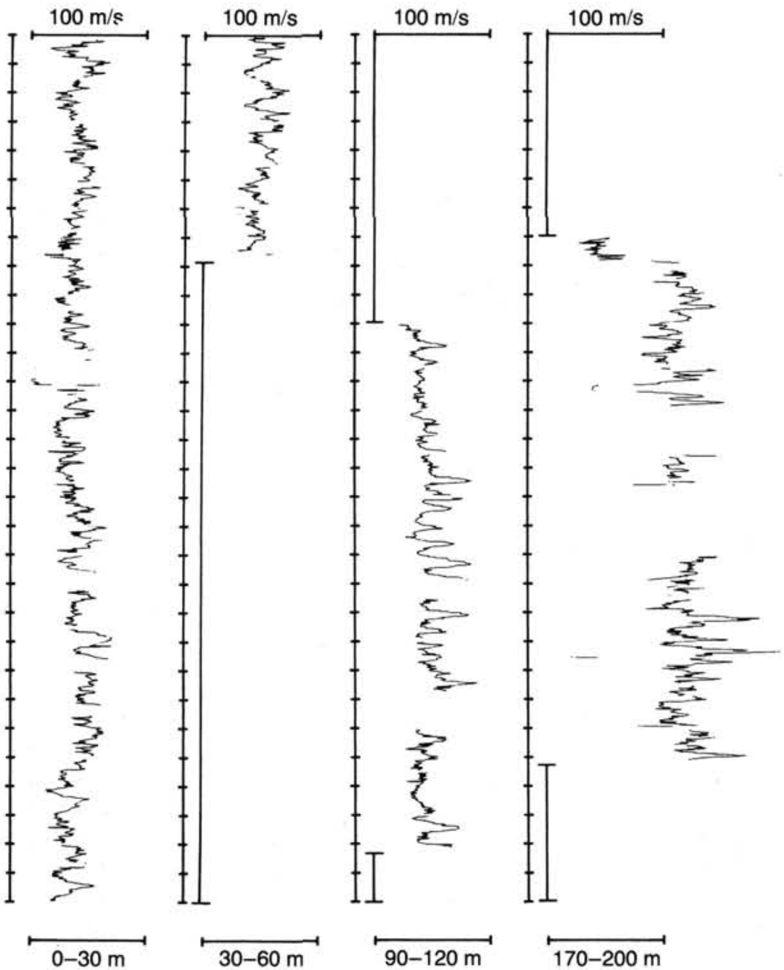

Figure 5. *P*-wave log for Hole 659C.

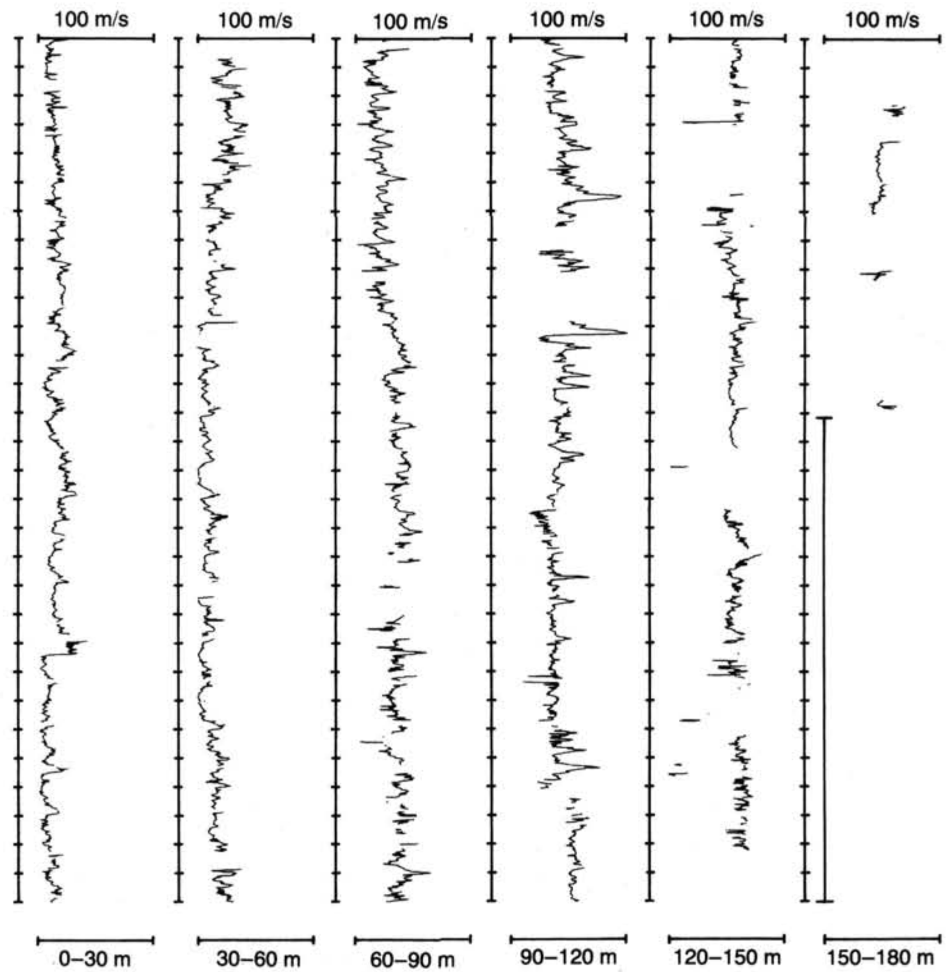

Figure 6A. *P*-wave log for Hole 660A.

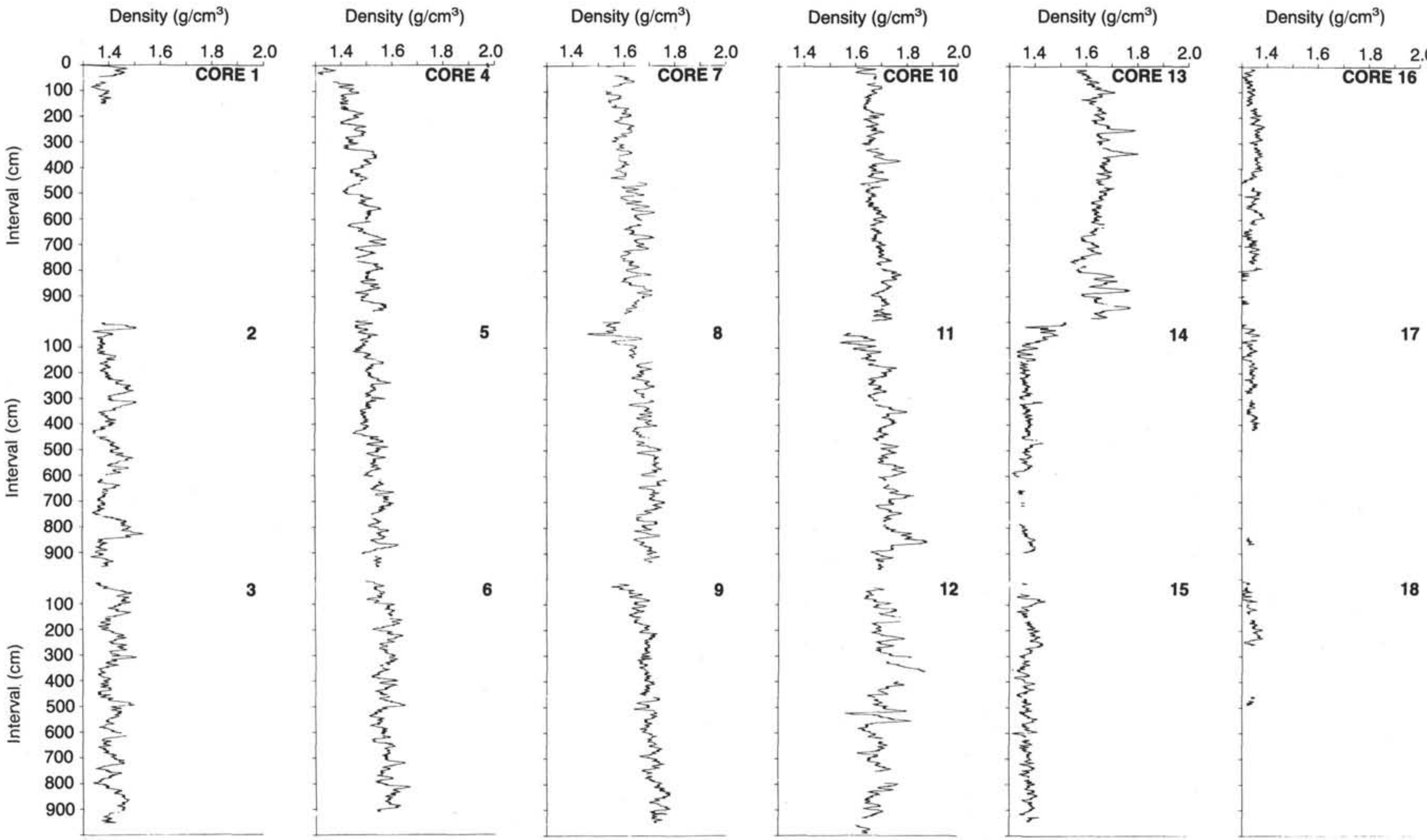

Figure 6B. Bulk-density log for Hole 660A.

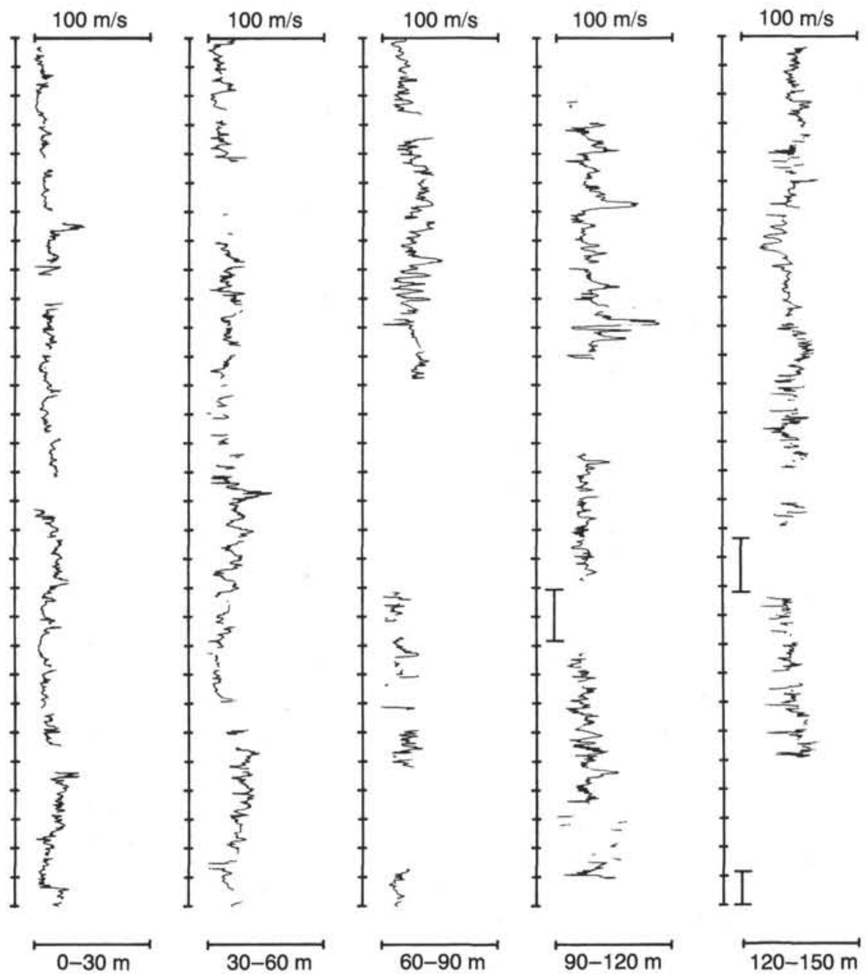

Figure 7. *P*-wave log for Hole 660B.

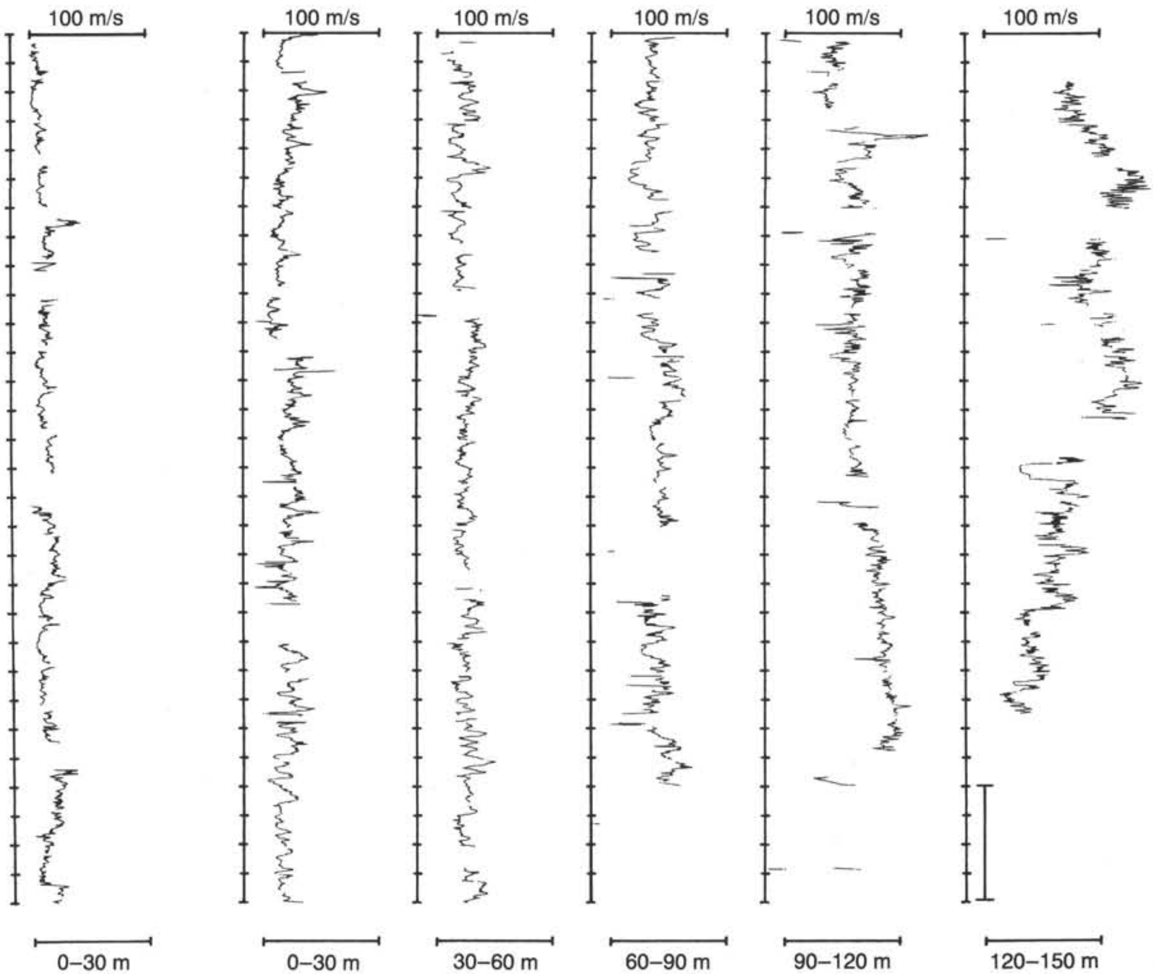

Figure 8A. *P*-wave log for Hole 661A.

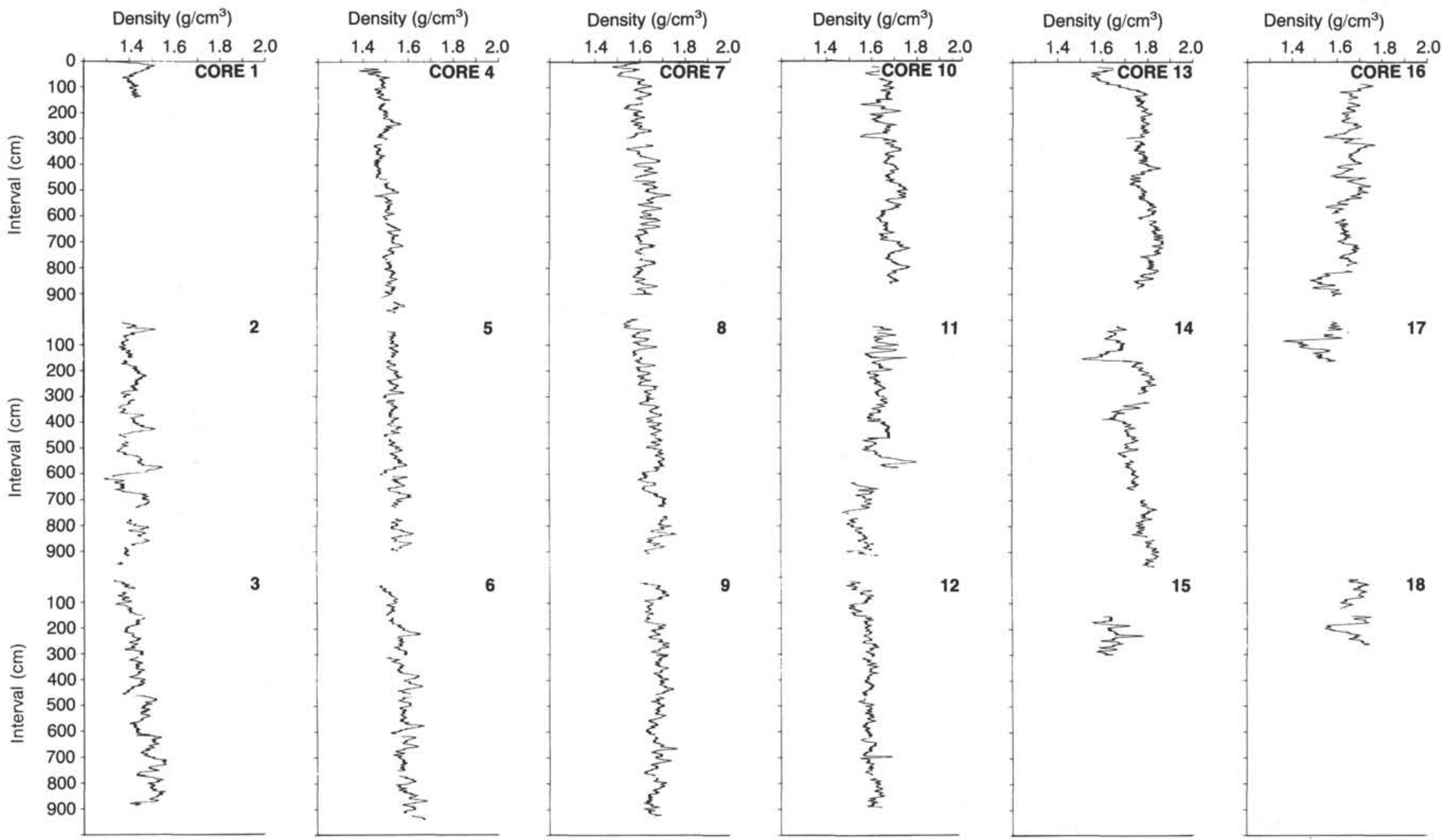

Figure 8B. Bulk-density log for Hole 661A.

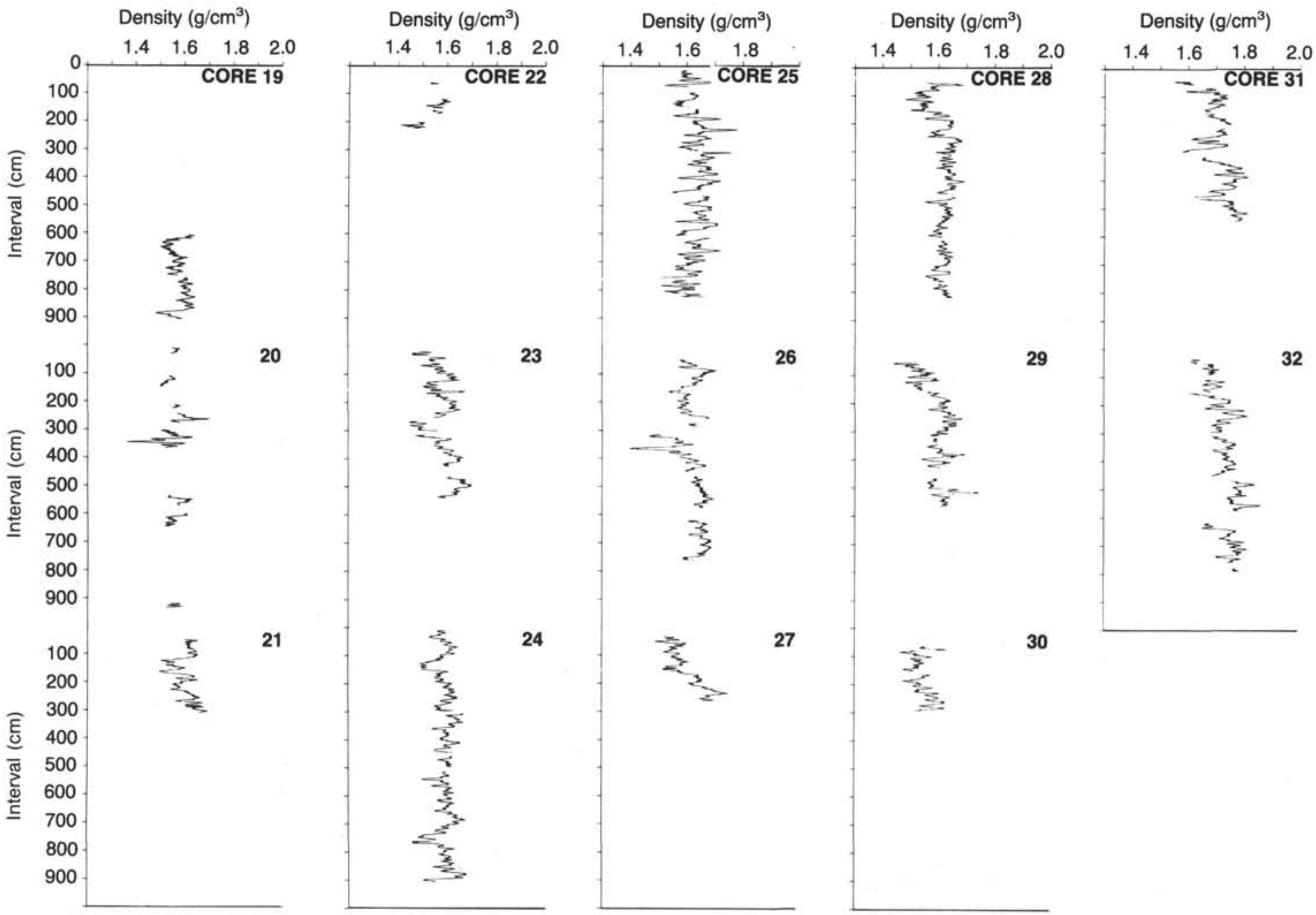

Figure 8B (continued).

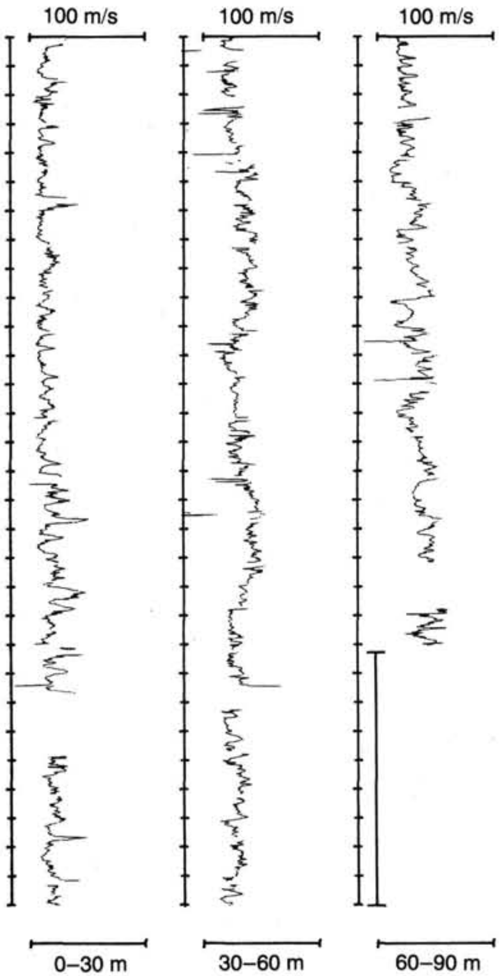

Figure 9. *P*-wave log for Hole 661B.

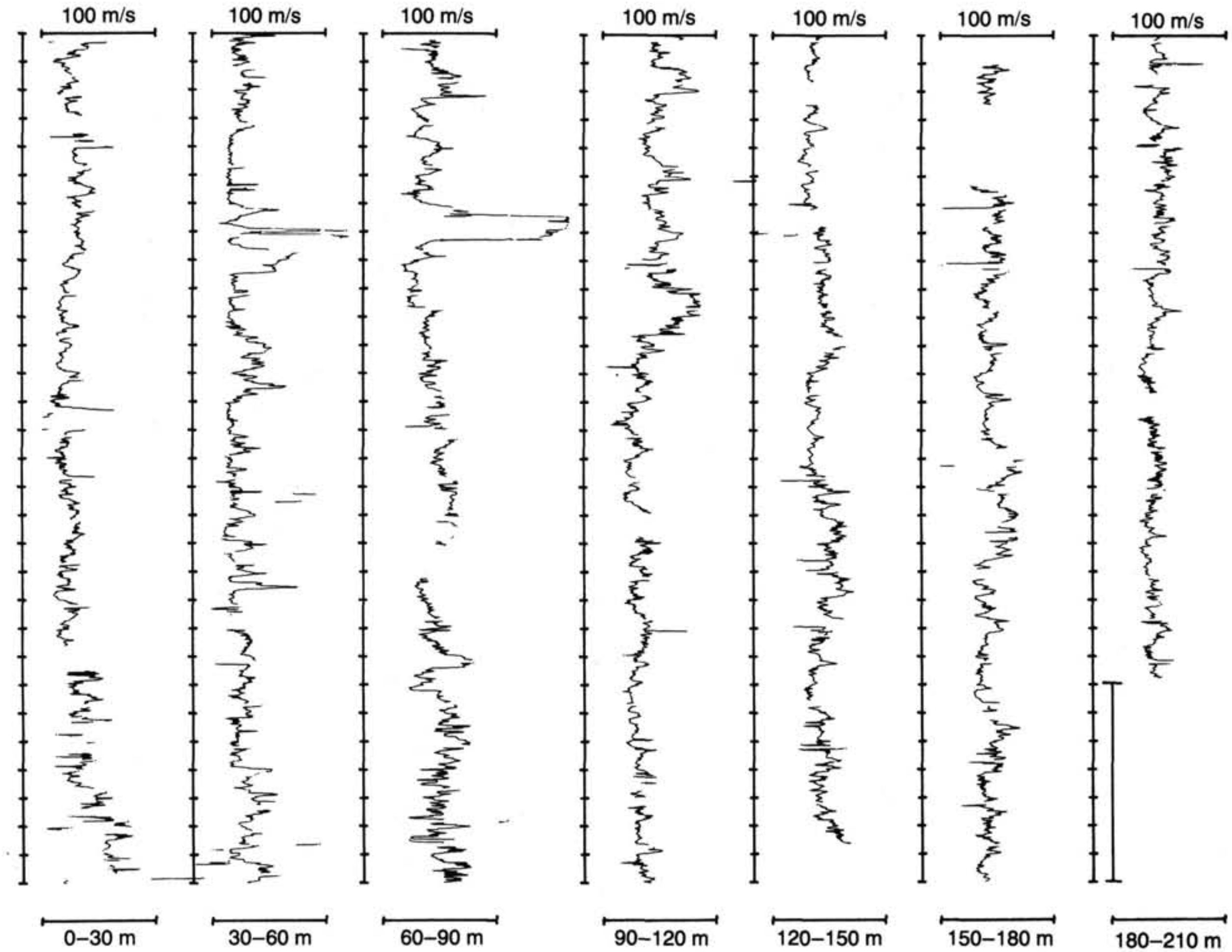

Figure 10A. *P*-wave log for Hole 662A.

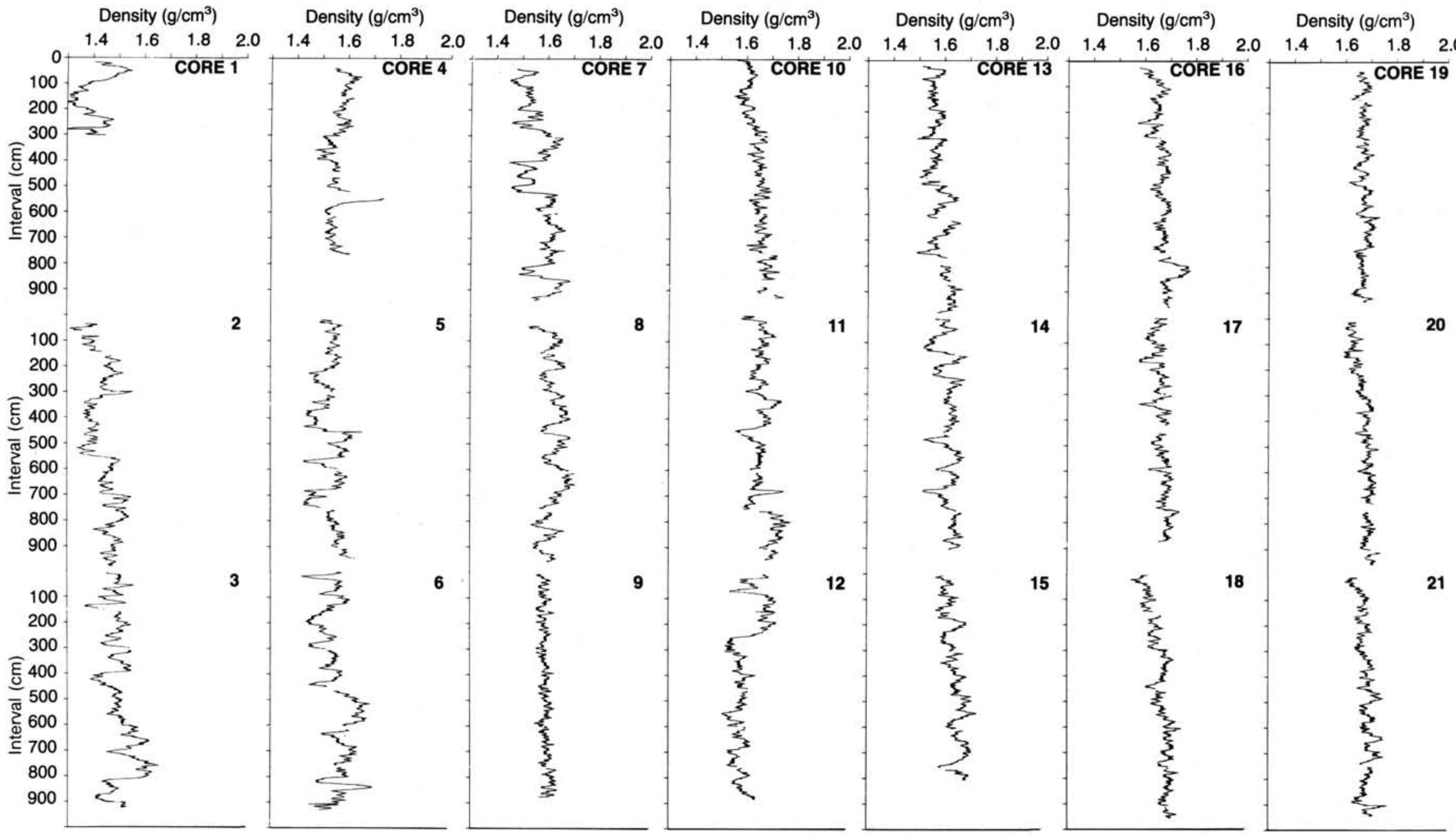

Figure 10B. Bulk-density log for Hole 662A.

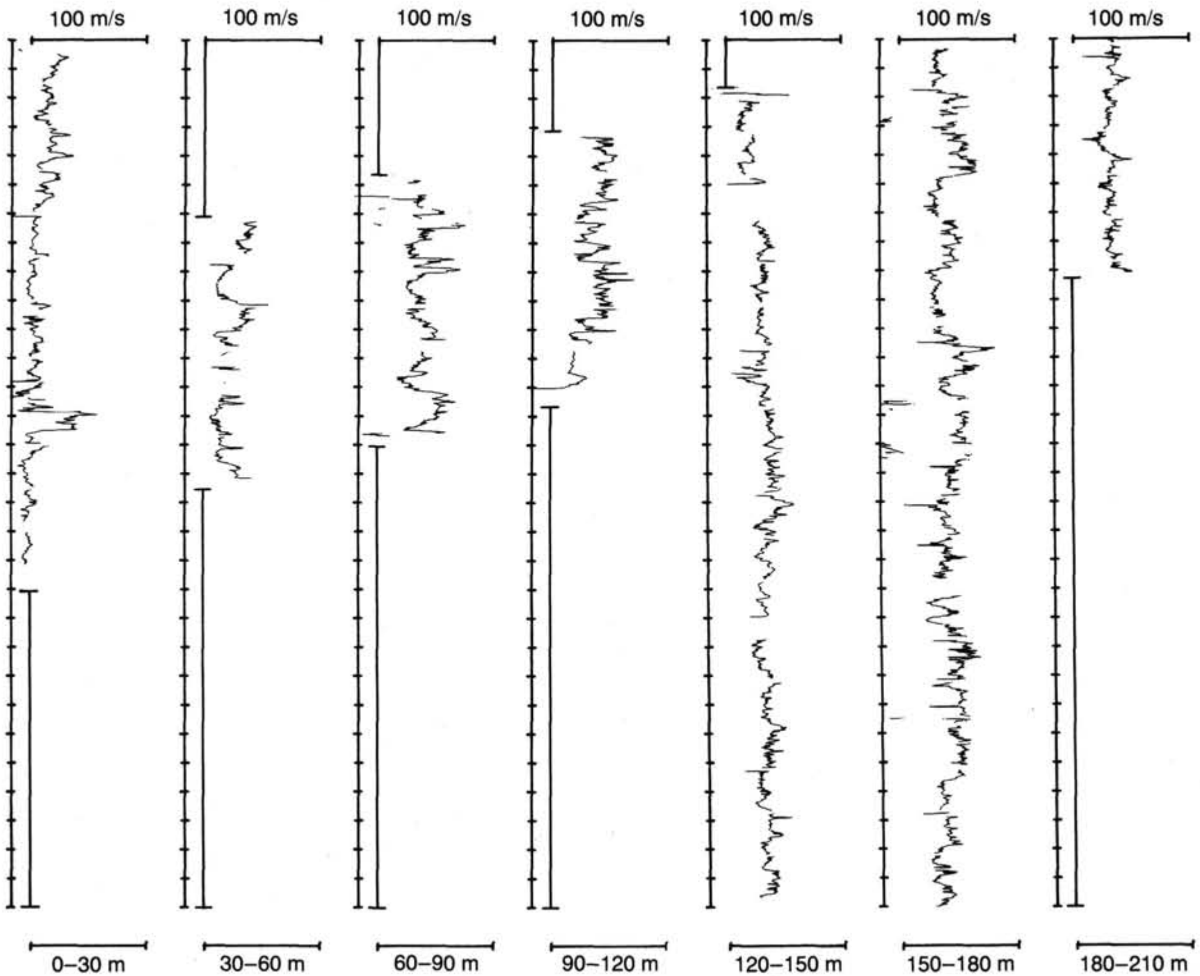

Figure 11. *P*-wave log for Hole 662B.

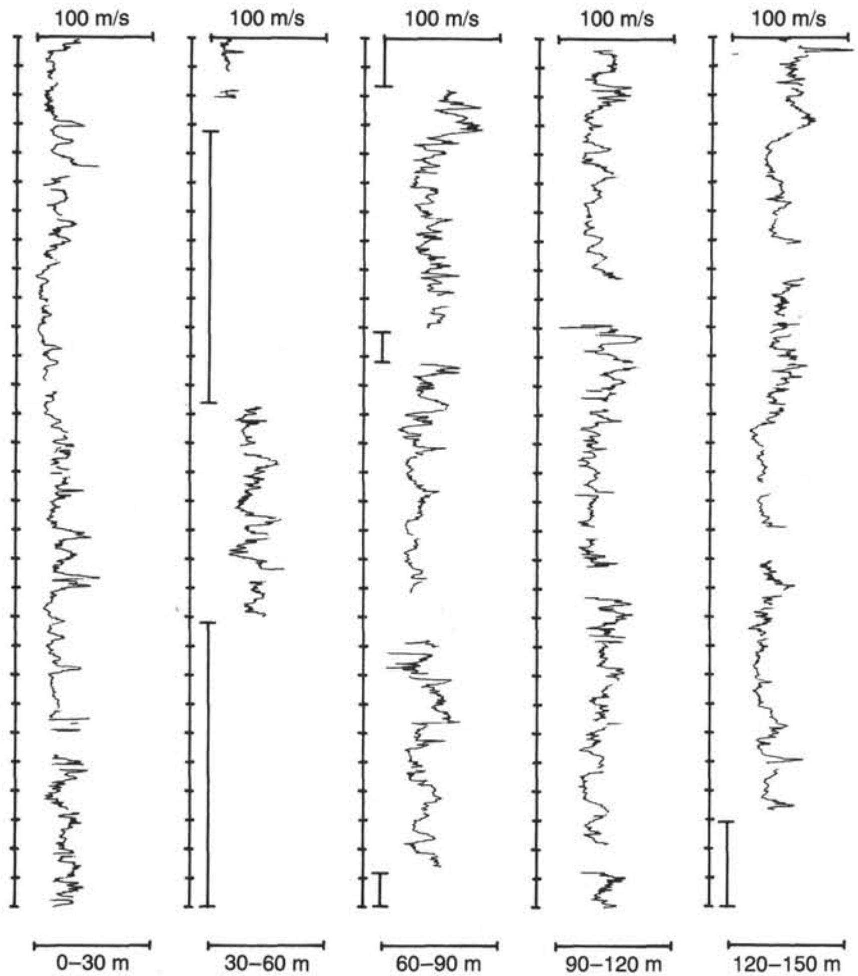

Figure 12A. *P*-wave log for Hole 663A.

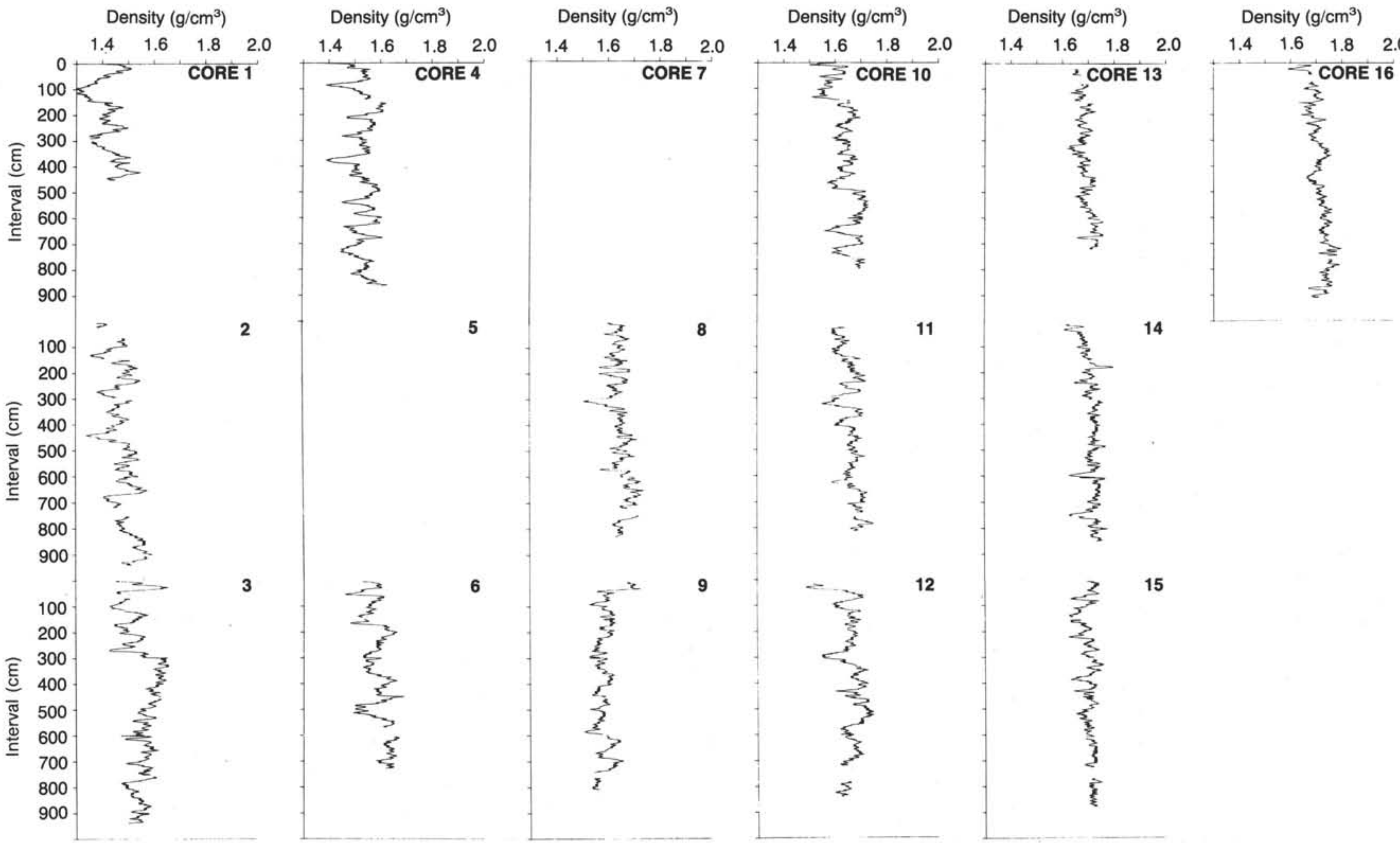

Figure 12B. Bulk-density log for Hole 663A.

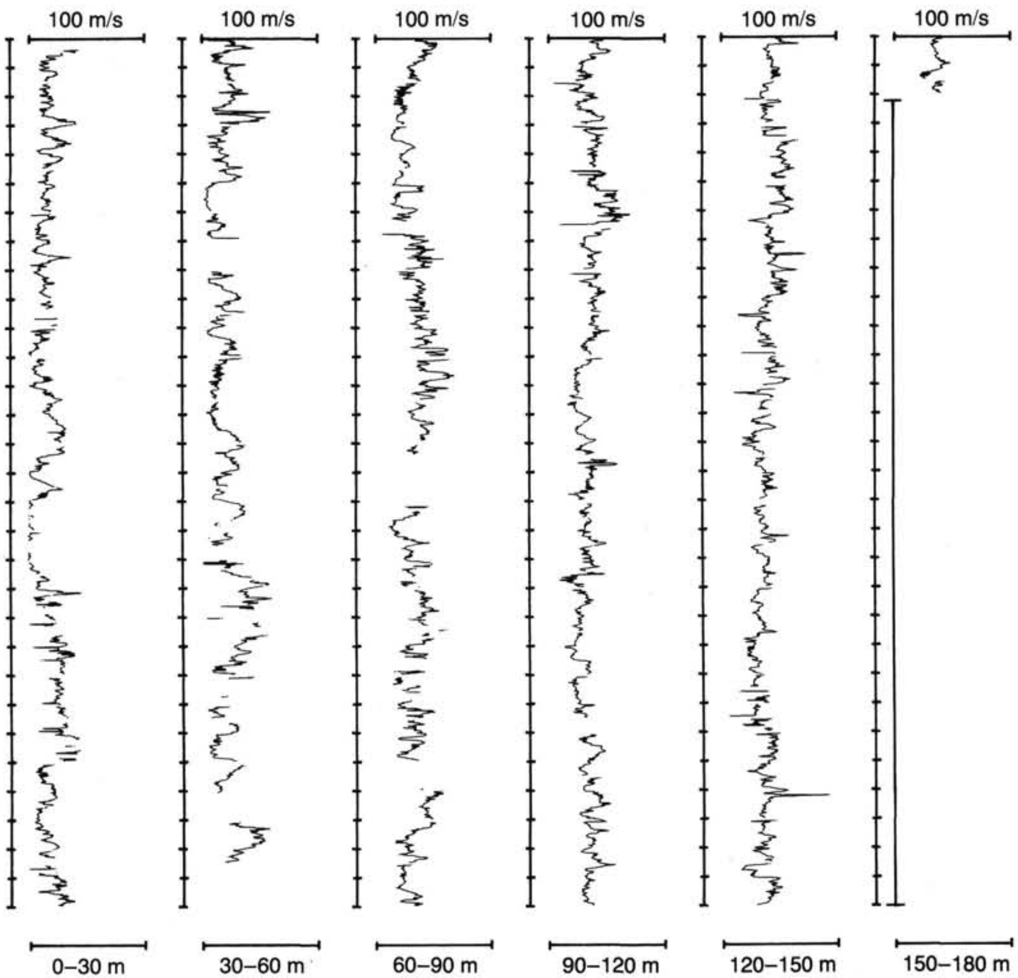

Figure 13. *P*-wave log for Hole 663B.

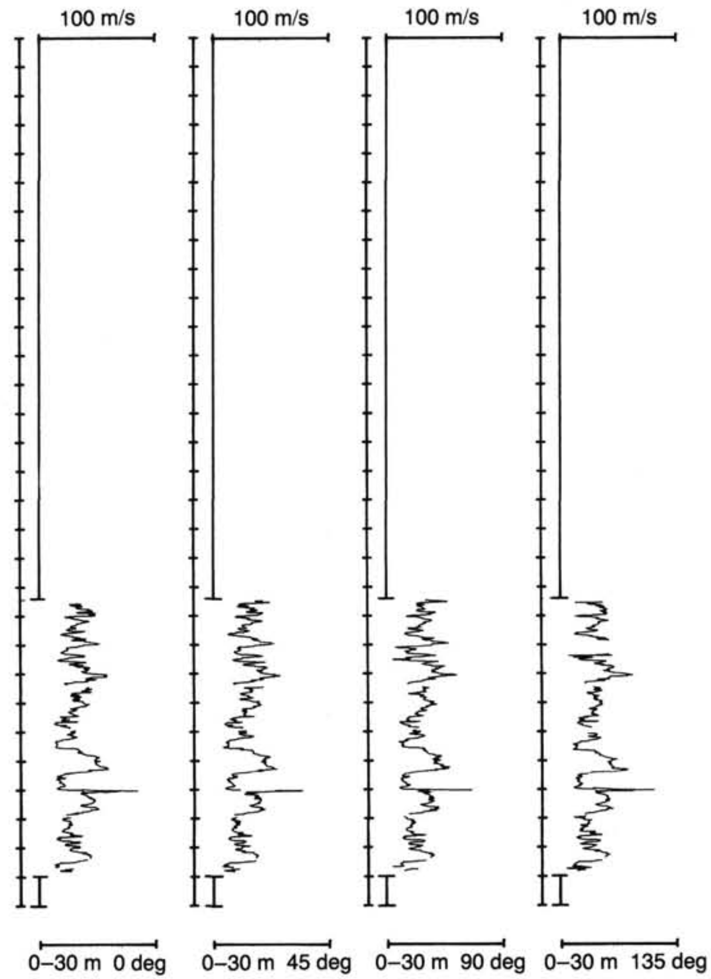

Figure 14. *P*-wave log for Hole 664A.

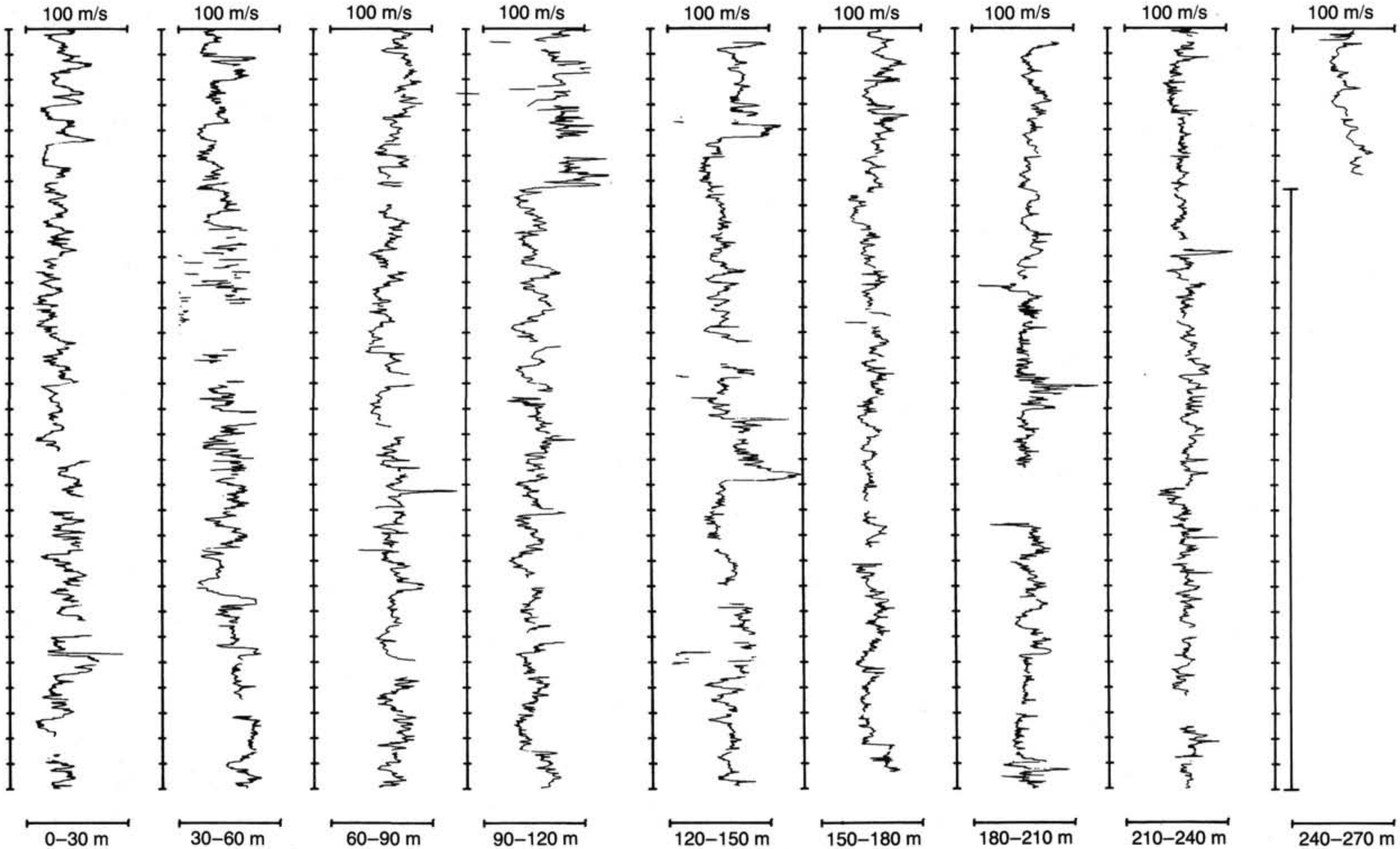

Figure 15A. *P*-wave log for Hole 664B.

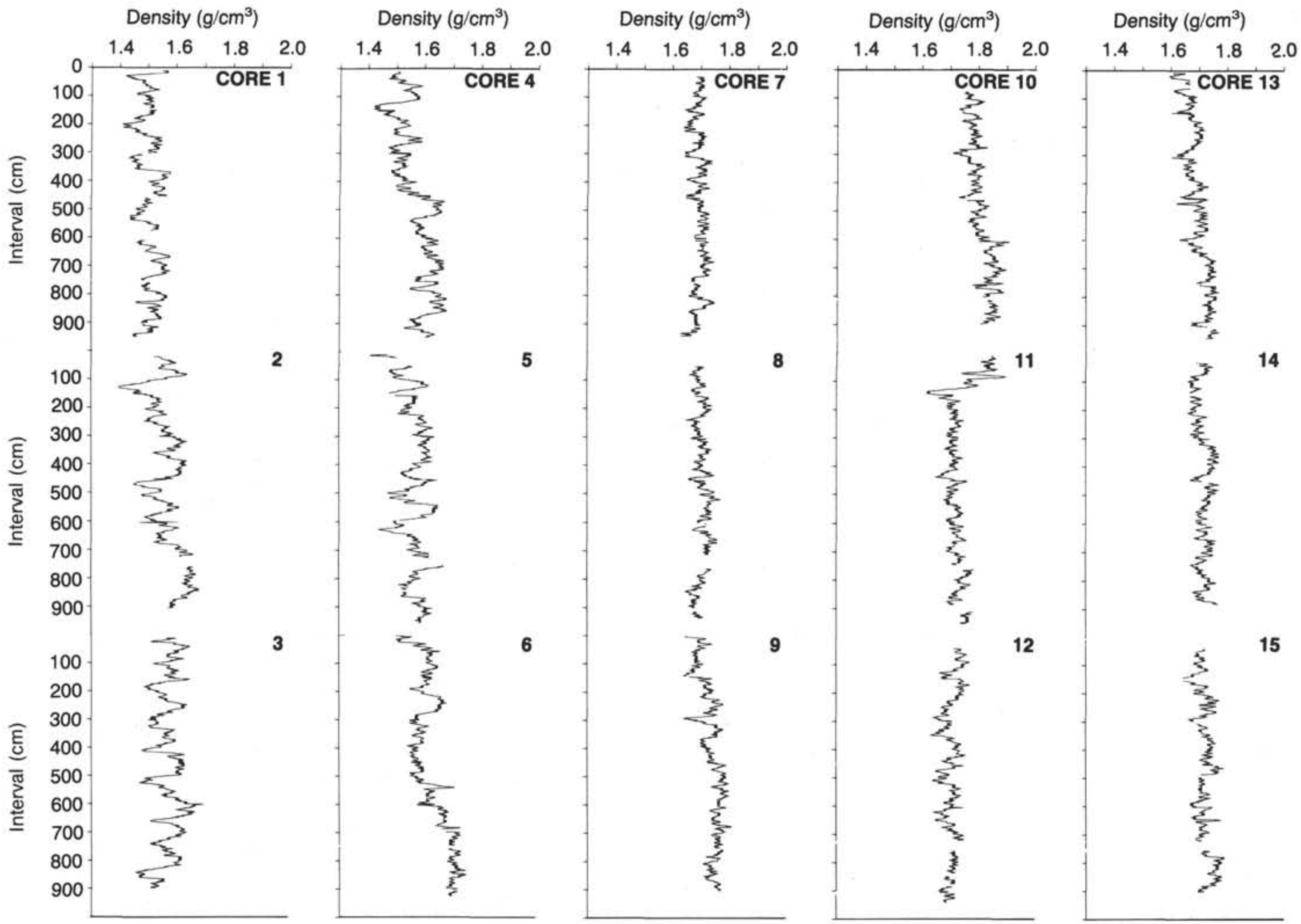

Figure 15B. Bulk-density log for Hole 664B.

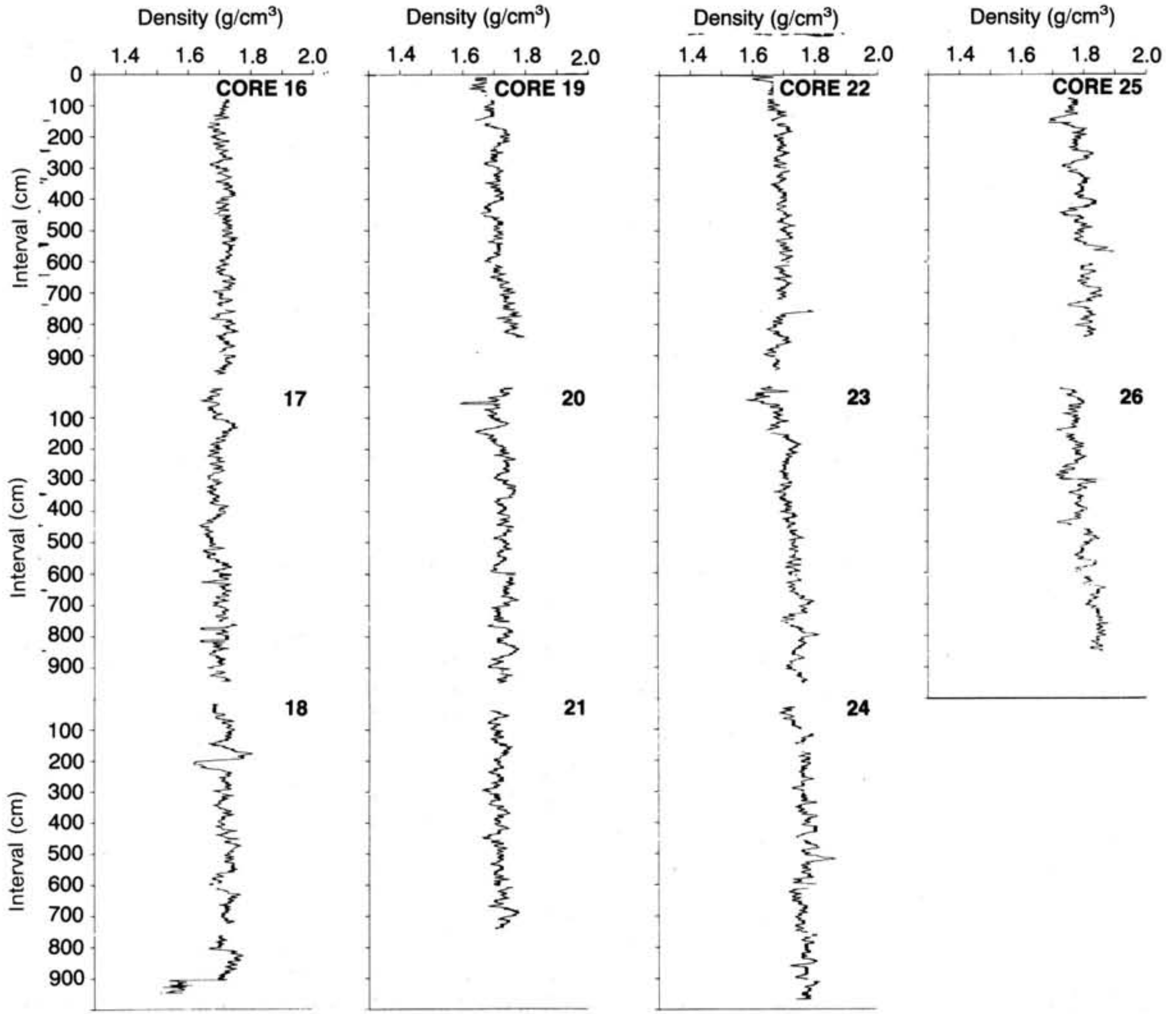

Figure 15B (continued).

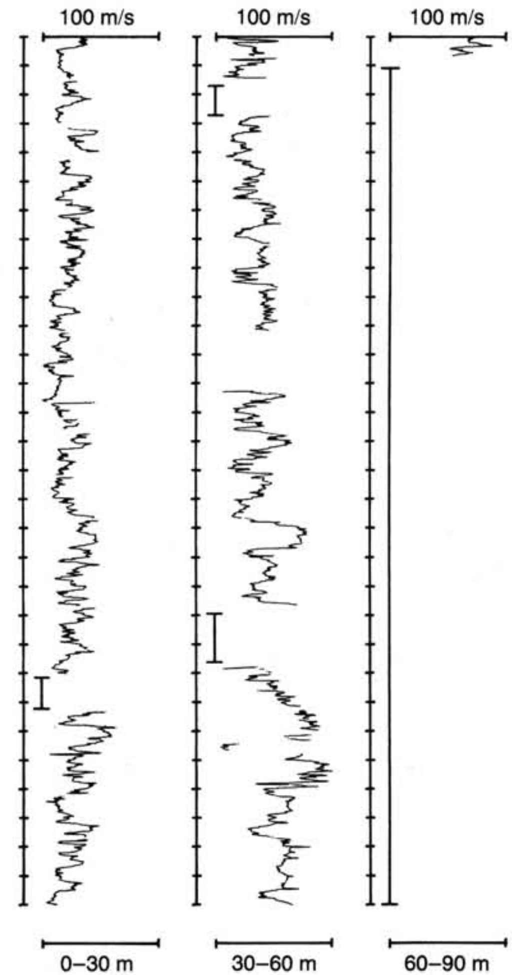

Figure 16. *P*-wave log for Hole 664C.

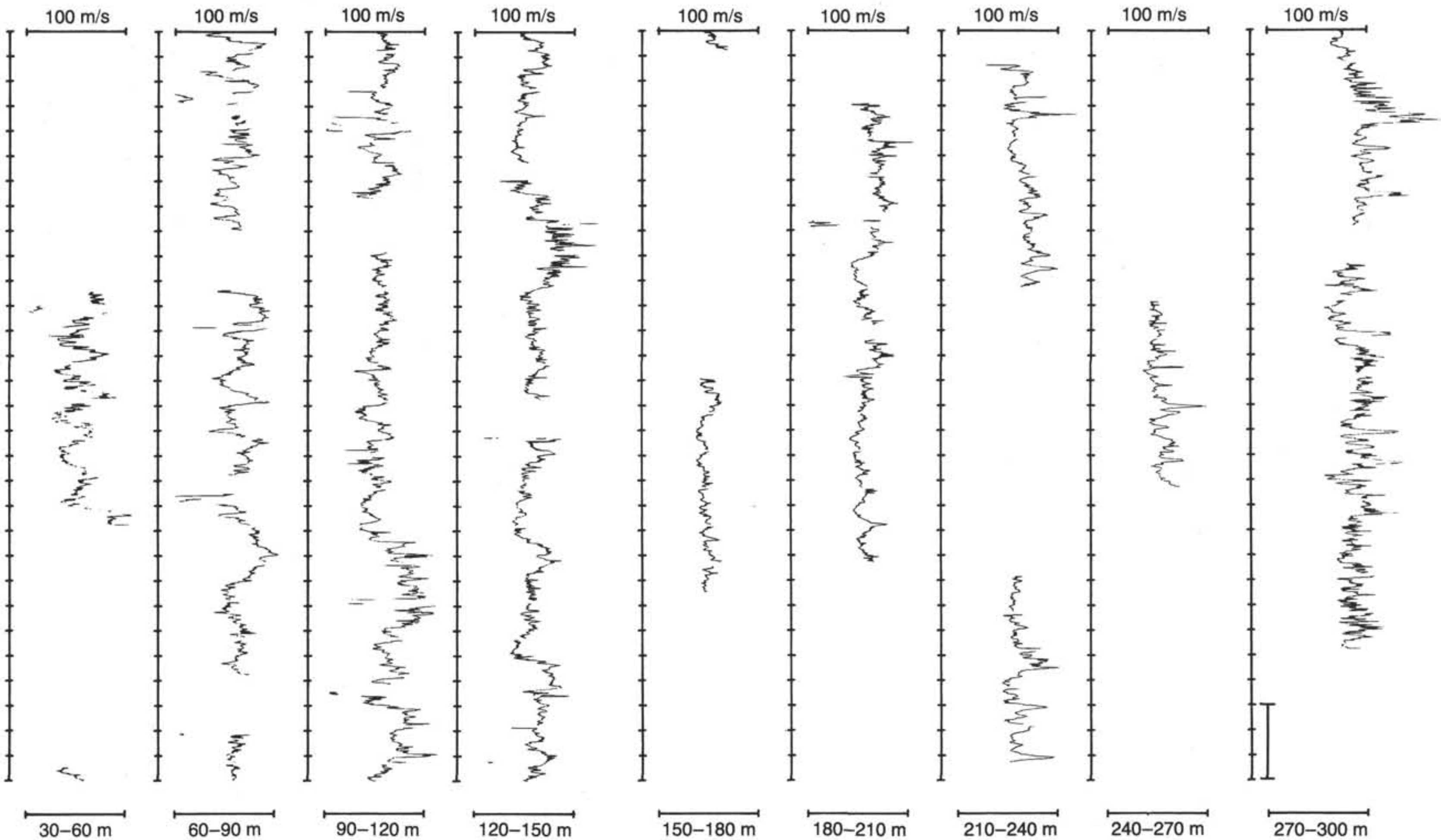

Figure 17. *P*-wave log for Hole 664D.

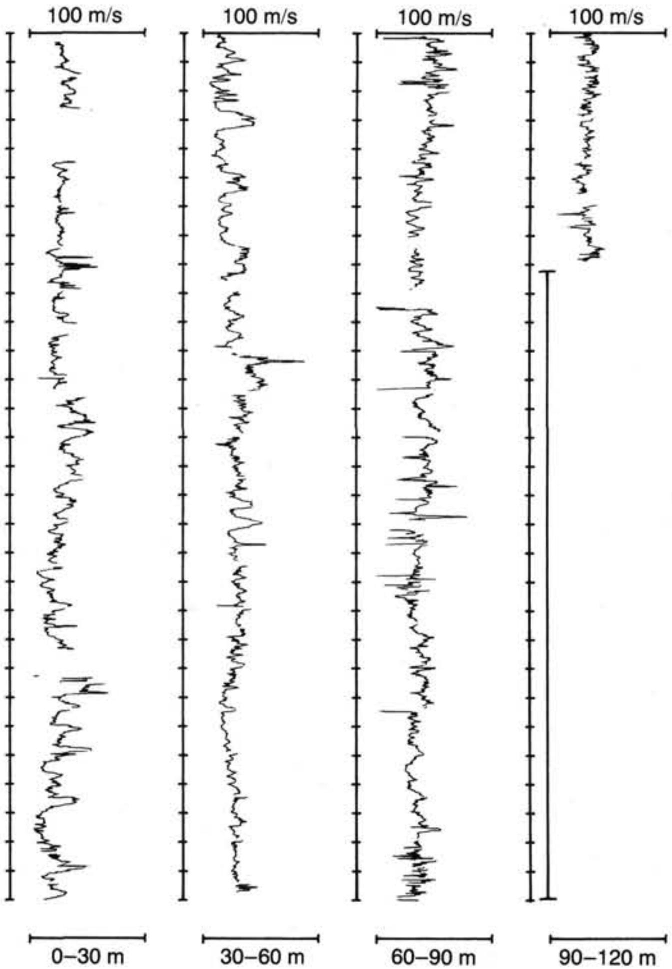

Figure 18A. *P*-wave log for Hole 665A.

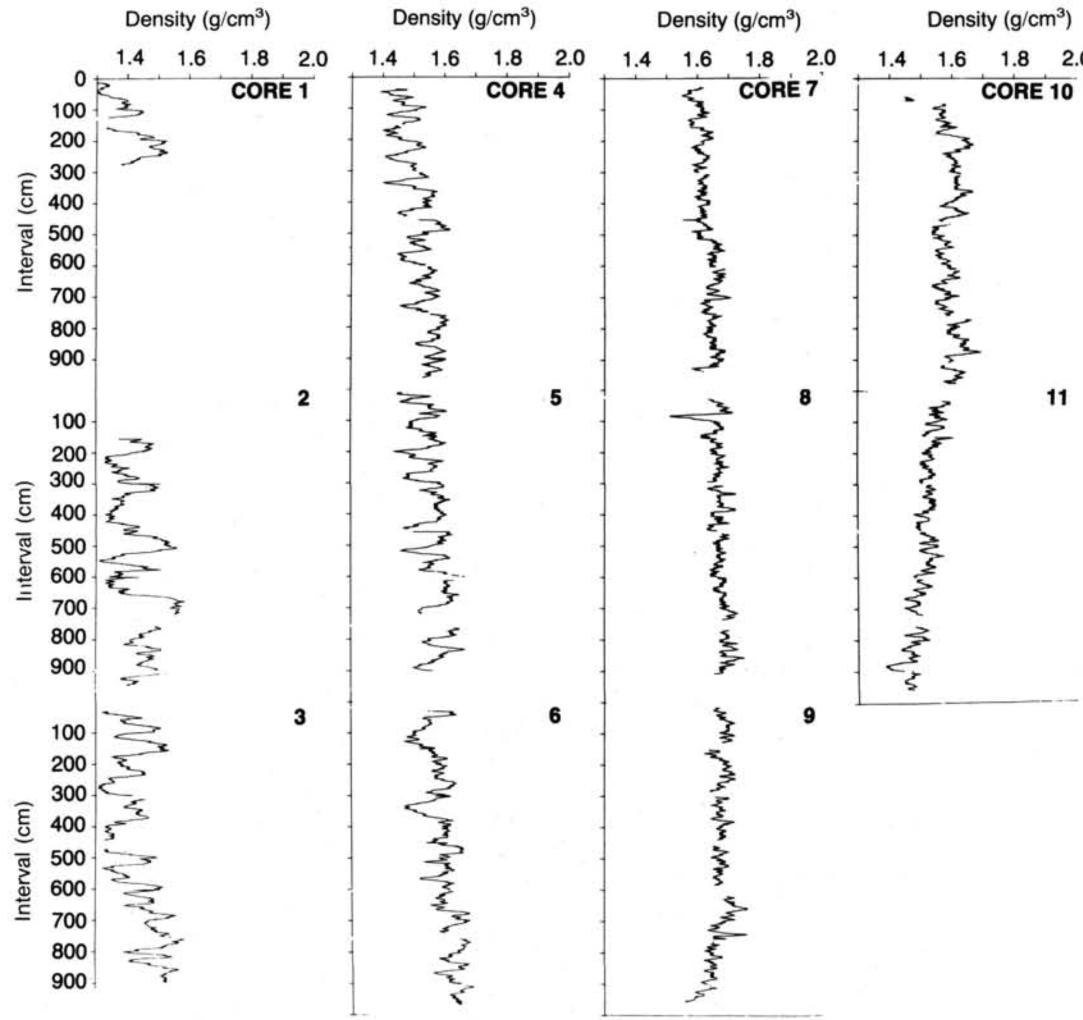

Figure 18B. Bulk-density log for Hole 665A.

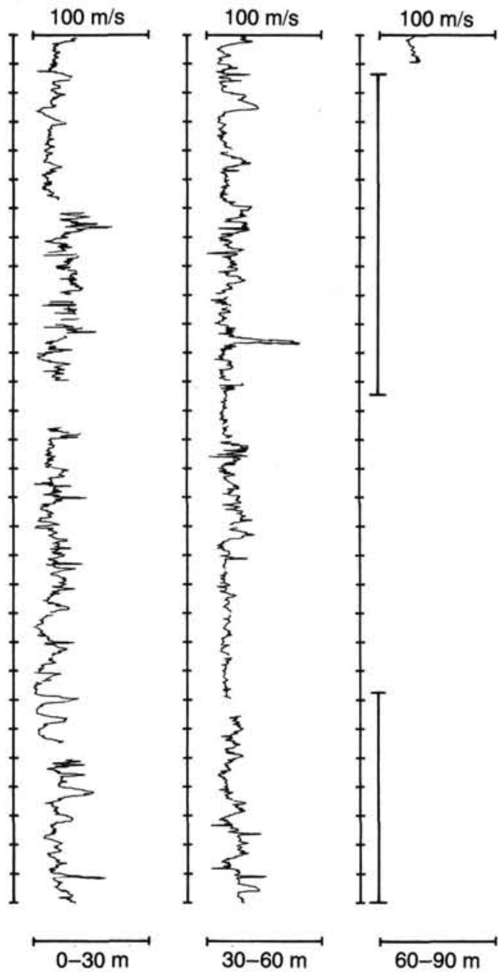

Figure 19. *P*-wave log for Hole 665B.

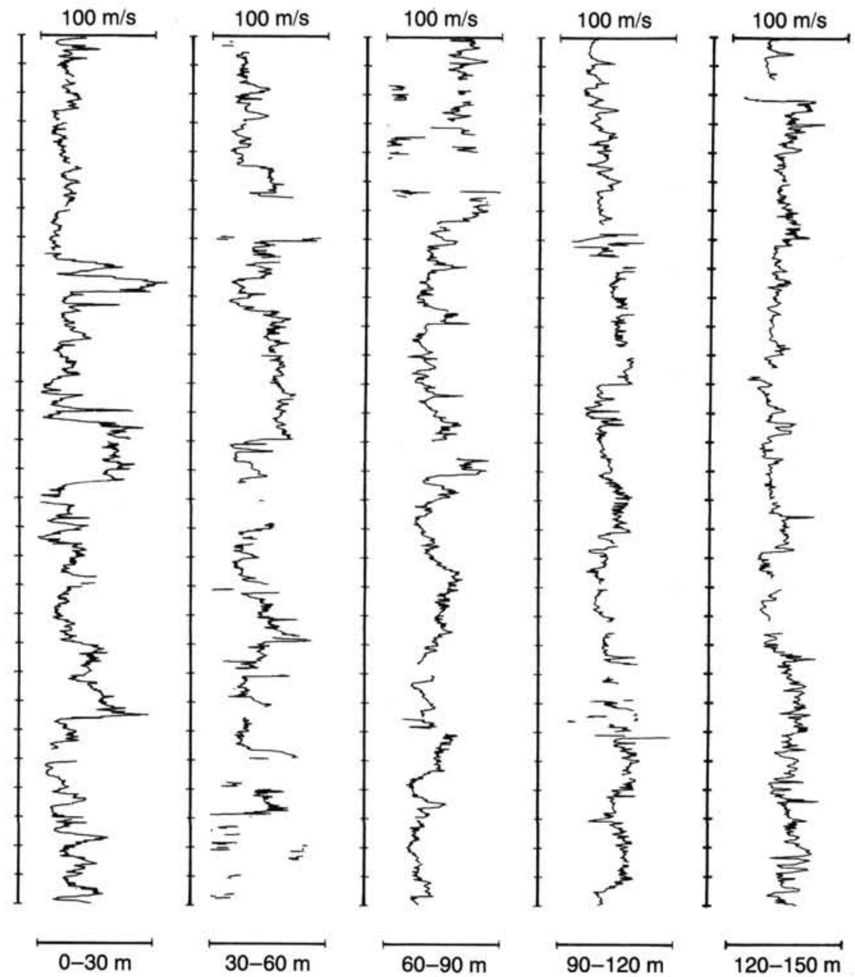

Figure 20A. *P*-wave log for Hole 666A.

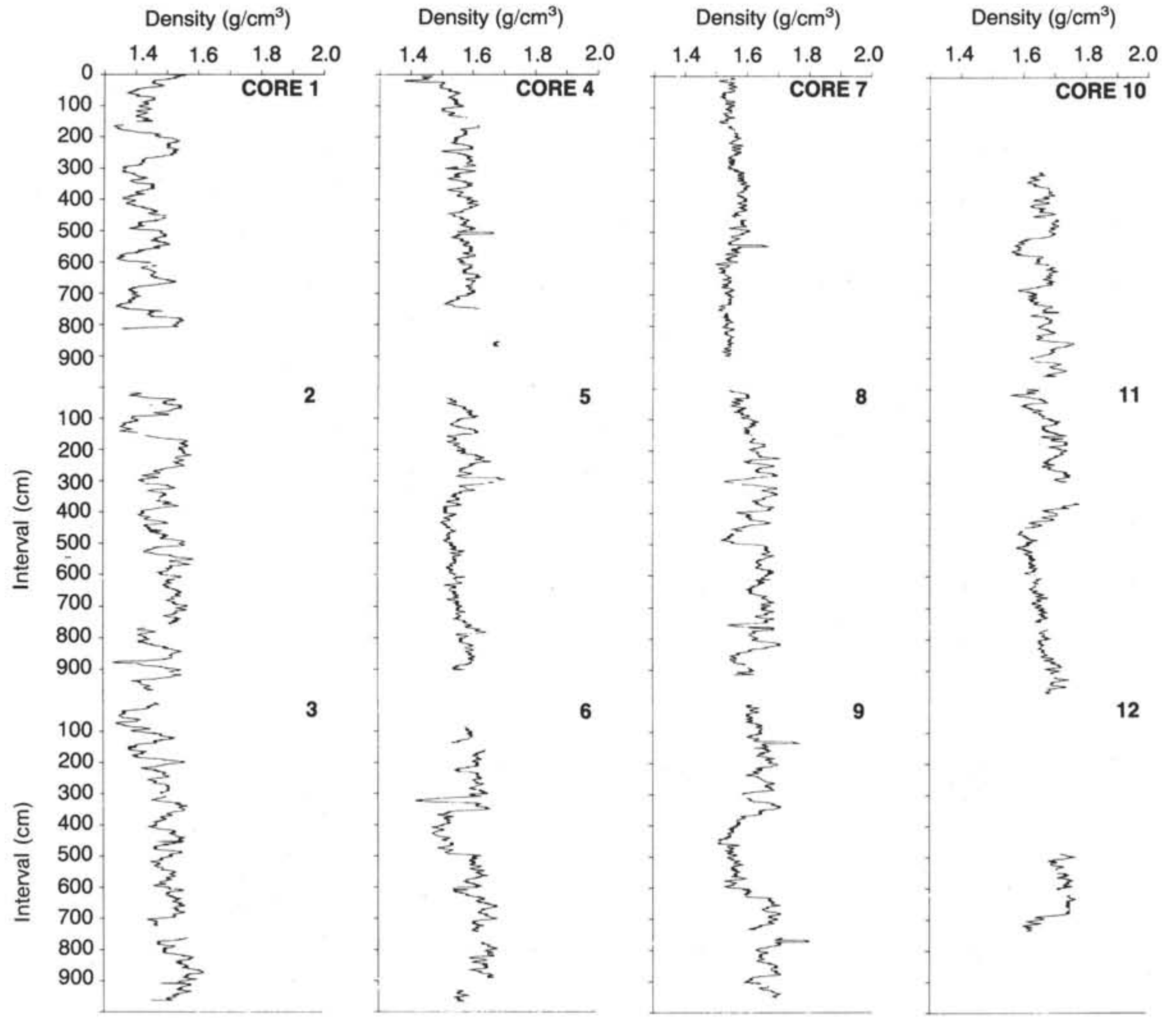

Figure 20B. Bulk-density log for Hole 666A.

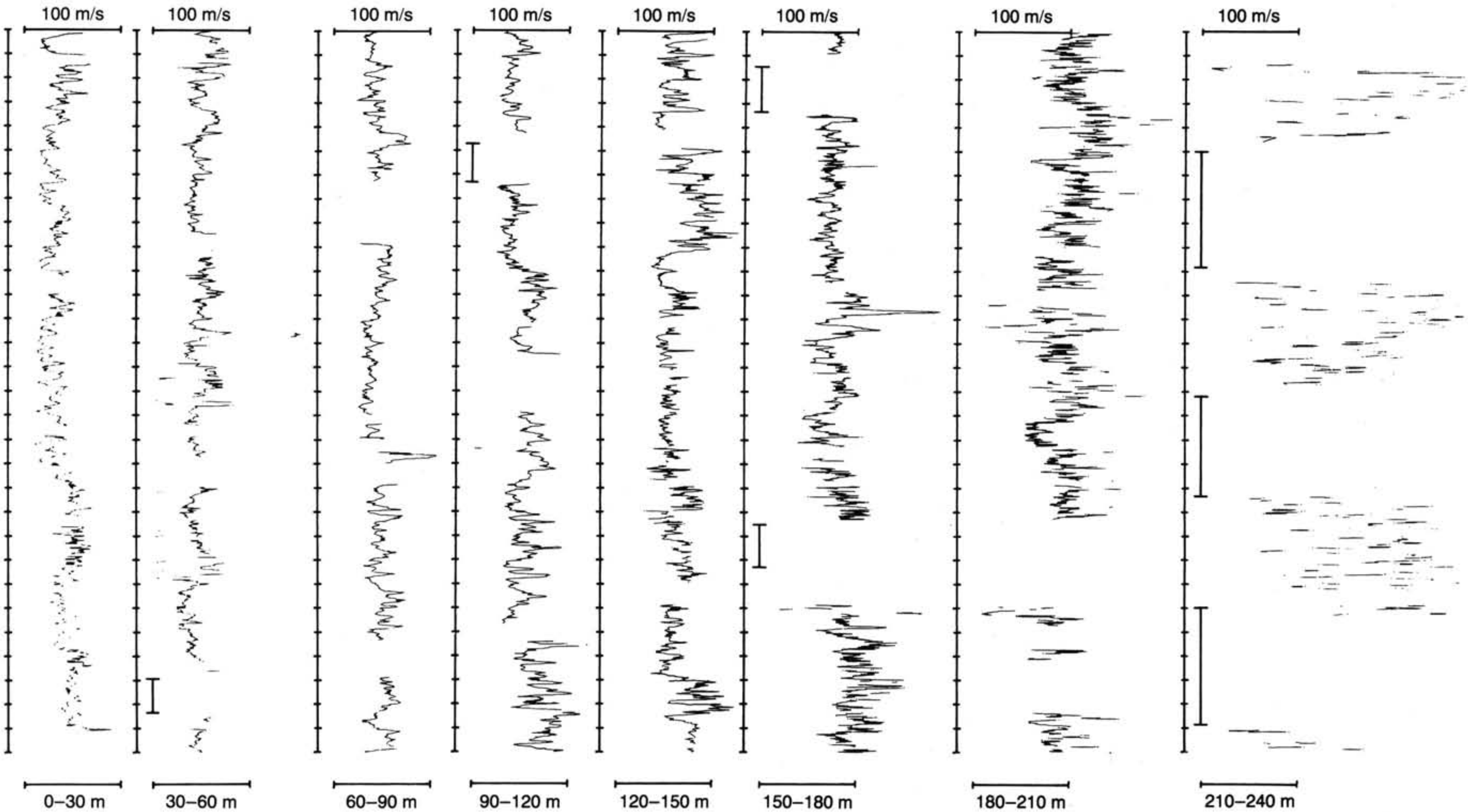

Figure 21A. *P*-wave log for Hole 667A.

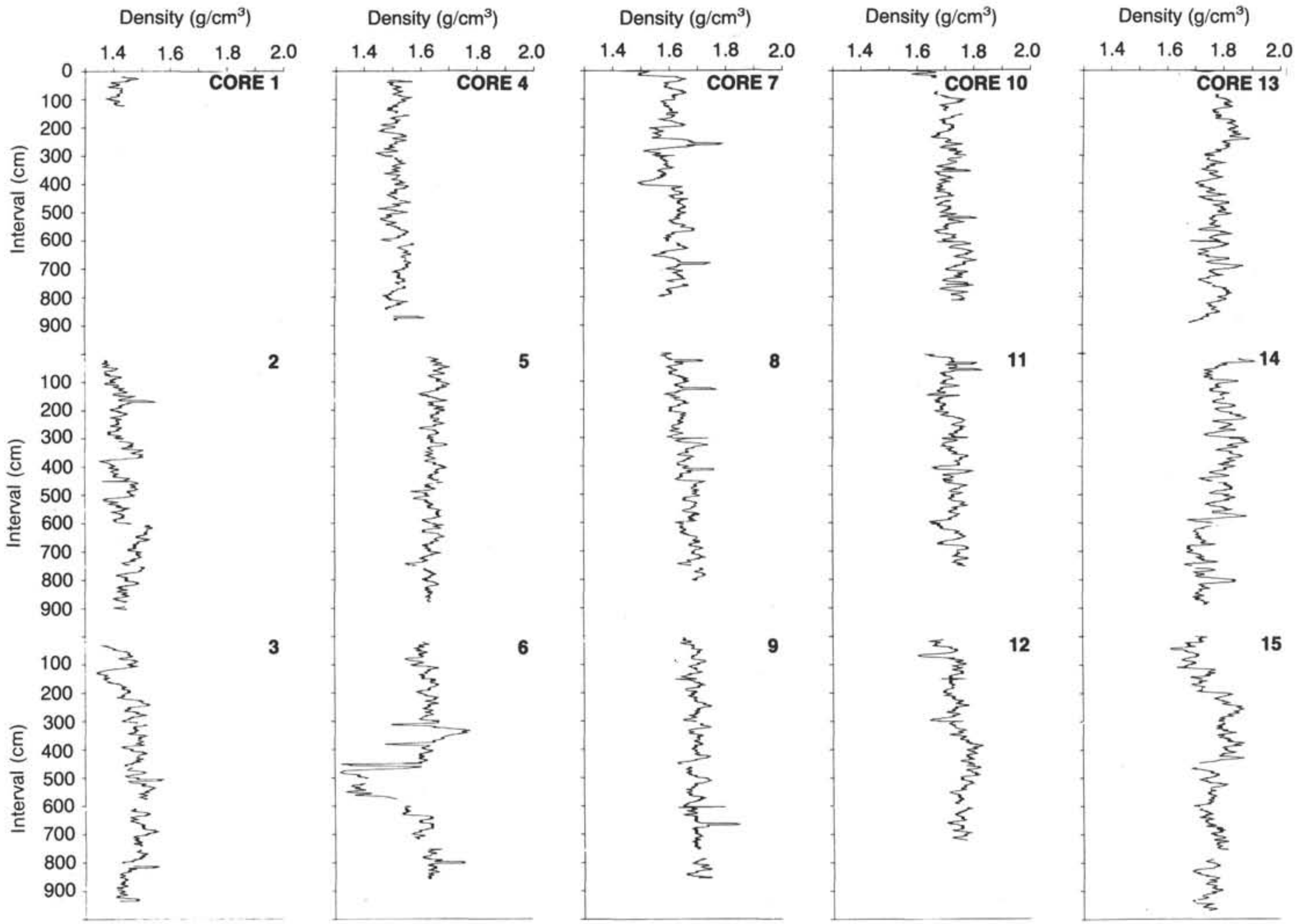

Figure 21B. Bulk-density log for Hole 667A.

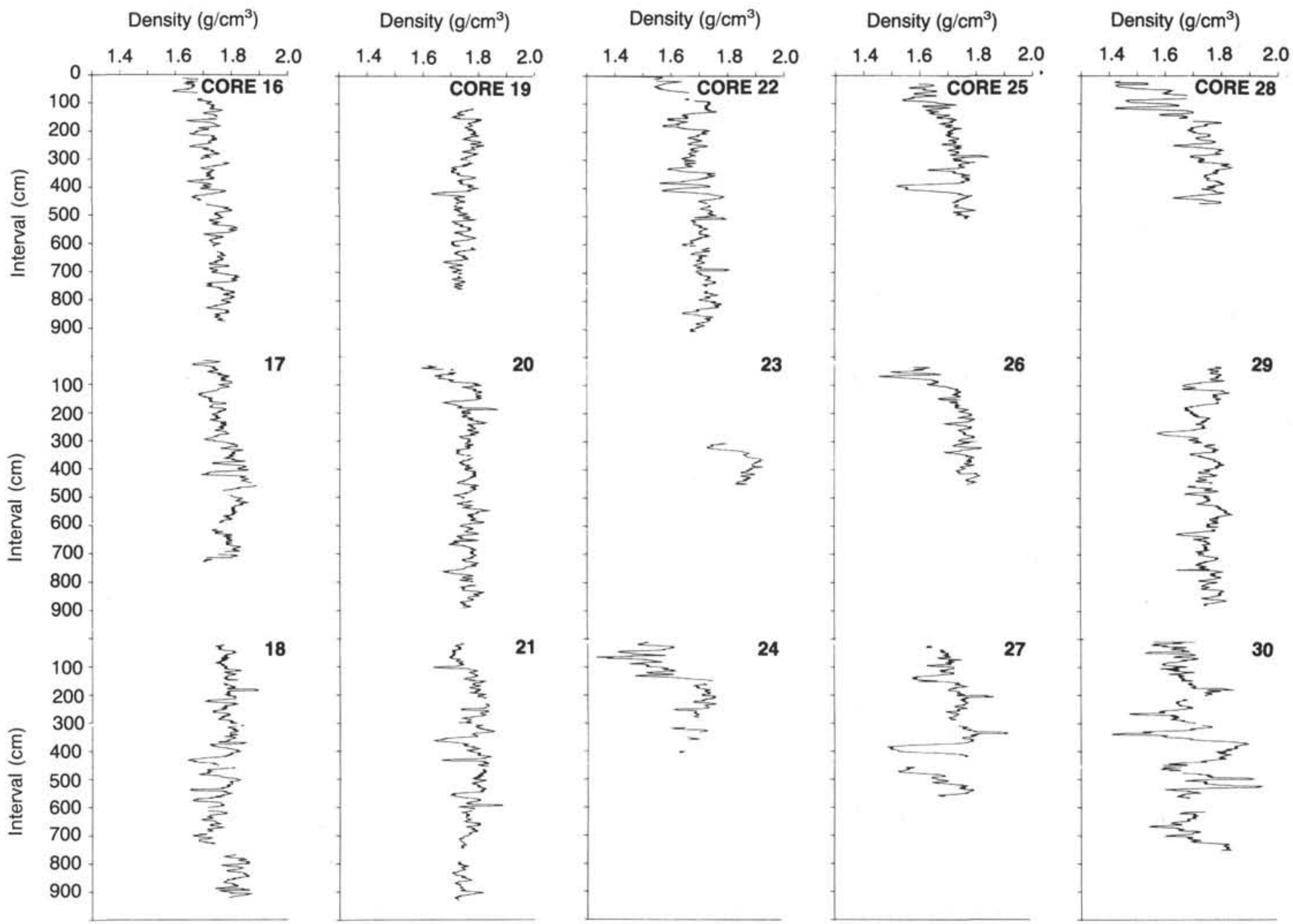

Figure 21B (continued).

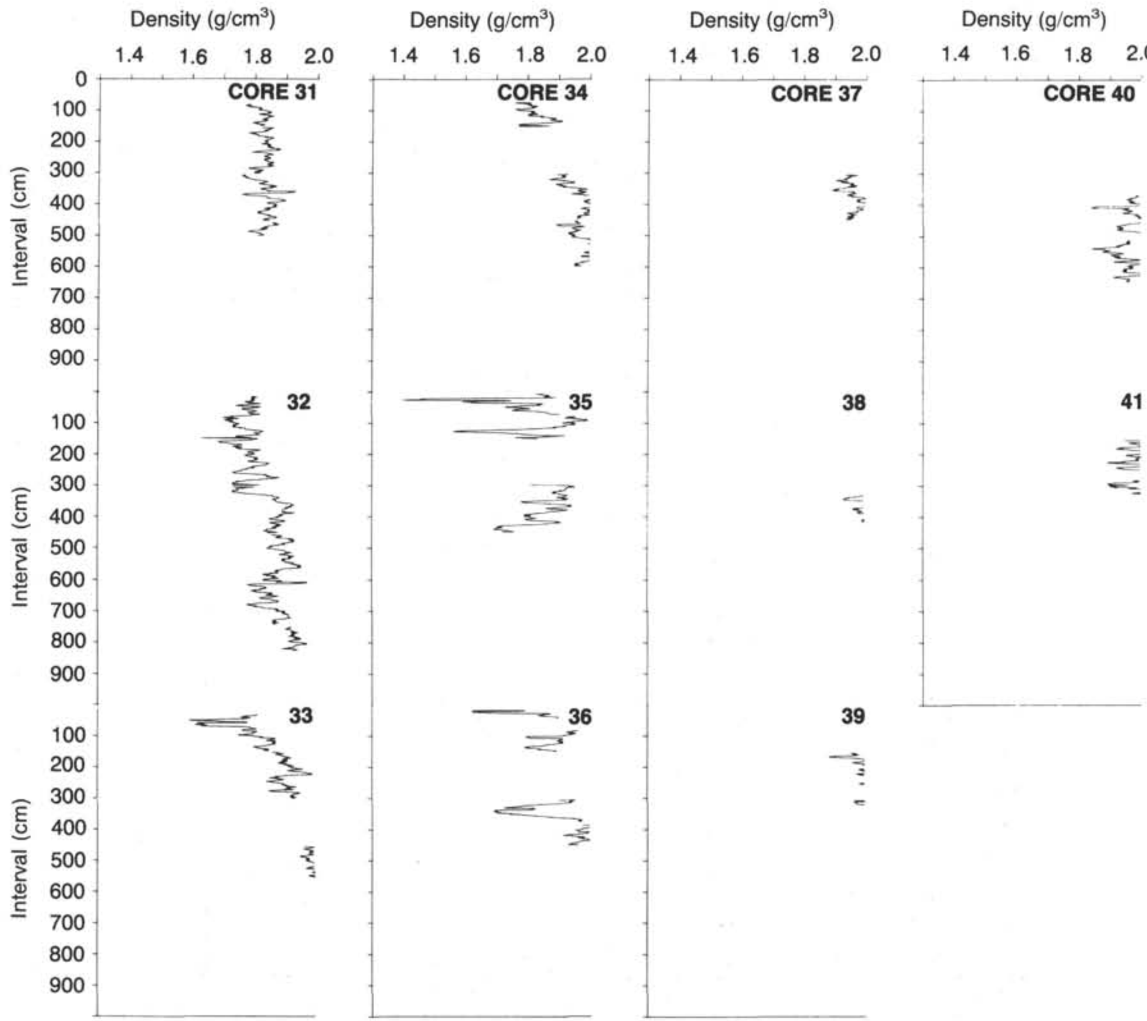

Figure 21B (continued).

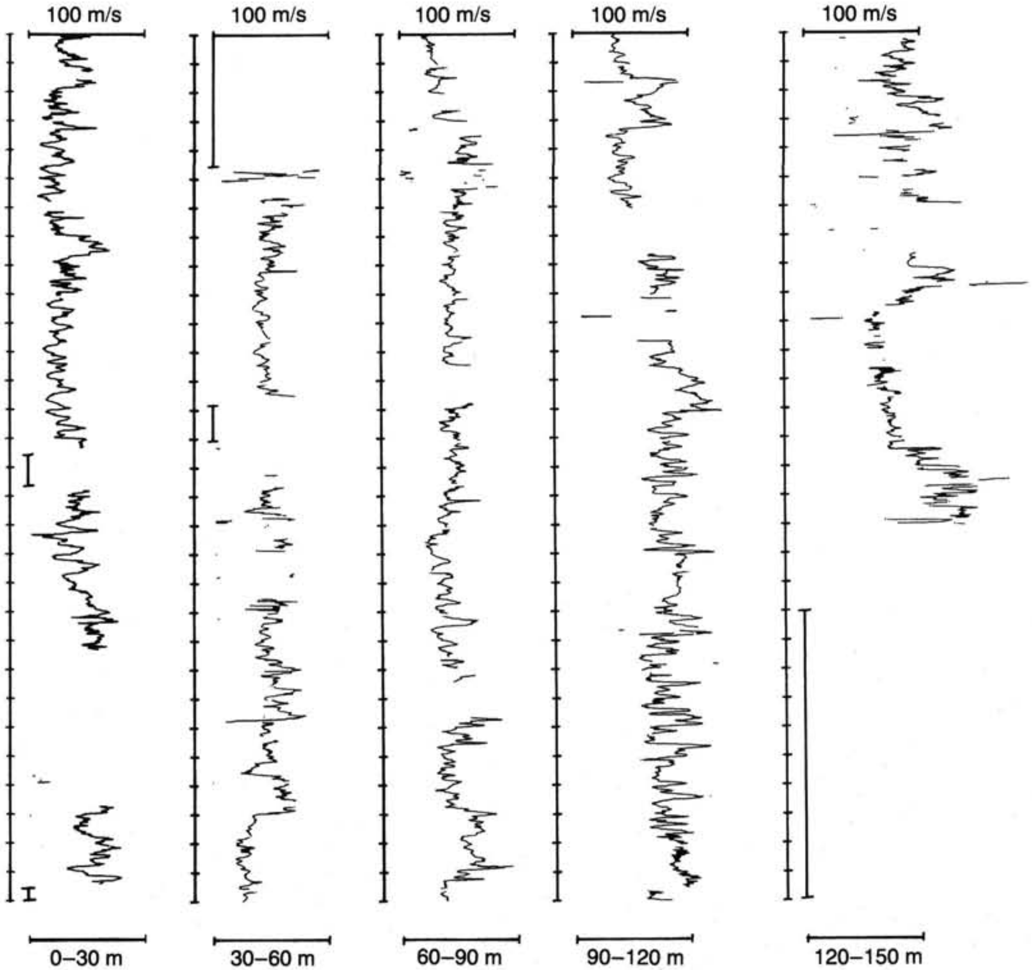

Figure 22. *P*-wave log for Hole 667B.

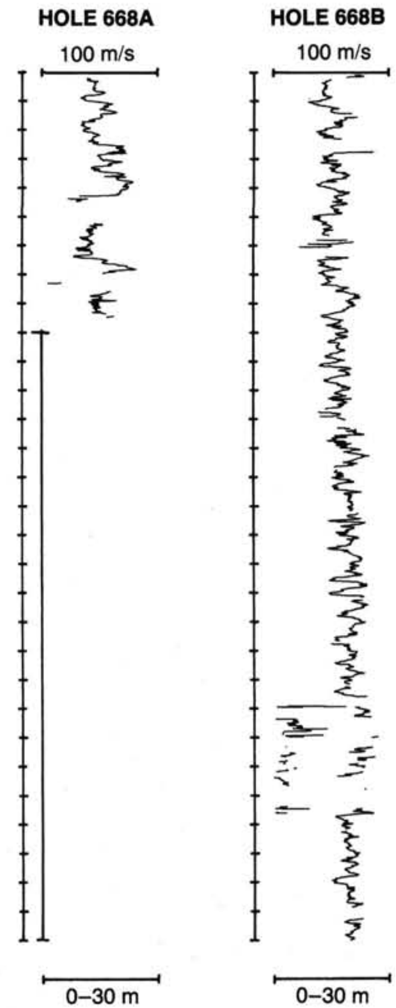

Figure 23. *P*-wave log for Holes 668A and 668B.